Journal of Phonetics 77 (2019) 100921

Contents lists available at ScienceDirect

Journal of Phonetics

journal homepage: www.elsevier.com/locate/Phonetics

Research Article

# Articulatory characterization of English liquid-final rimes

Michael Proctor[a,*], Rachel Walker[b], Caitlin Smith[b], Tünde Szalay[c], Louis Goldstein[b], Shrikanth Narayanan[b]

[a] Department of Linguistics, Centre for Language Sciences, Macquarie University, Australia
[b] Department of Linguistics, University of Southern California, United States
[c] Department of Linguistics, Macquarie University, Australia

ARTICLE INFO

*Article history:*
Received 26 February 2018
Received in revised form 29 August 2019
Accepted 15 September 2019
Available online 23 October 2019

*Keywords:*
Liquid consonant
Rhotic
Lateral
Coarticulation
Syllable structure

ABSTRACT

Articulation of liquid consonants in onsets and codas by four speakers of General American English was examined using real-time MRI. Midsagittal tongue posture was compared for laterals and rhotics produced in each syllable margin, adjacent to 13 different vowels and diphthongs. Vowel articulation was examined in words without liquids, before each liquid, and after each liquid, to assess the coarticulatory influence of each segment on the others. Overall, nuclear vocalic postures were more influenced by coda rhotics than onset rhotics or laterals in either syllable margin. Laterals exhibited greater temporal and spatial independence between coronal and dorsal gestures. Rhotics were produced with a variety of speaker-specific postures, but were united by a greater degree of coarticulatory resistance to vowel context, patterns consistent with greater coarticulatory influence on adjacent vowels, and less allophonic variation across syllable positions than laterals.



## 1. Introduction

Liquid consonants in American English exhibit asymmetries with respect to the range of contrasts in co-occurring vowels in the rime. Fewer vowel contrasts are attested before coda rhotics than laterals (Hammond, 1999; Proctor & Walker, 2012). For example, in General American English (Wells, 1982), tense and lax vowel contrasts, such as /i/-/ɪ/ and /eɪ/-/ɛ/, are neutralized before a coda rhotic, as in words like *'beer'* and *'bare'*, while the same contrasts are maintained before a coda lateral, as in words like *'peel'* versus *'pill'* (/i/-/ɪ/) and *'fail'* and *'fell'* (/eɪ/-/ɛ/). Nonetheless, neutralization of vowel contrasts preceding a coda lateral occurs in some varieties of American English, though with weaker effect than that of the rhotic. For example, in varieties of Southern American English, the /i/-/ɪ/ contrast is also neutralized before a coda lateral, and there is a weaker propensity for merger of the /eɪ/-/ɛ/ contrast in the same context (Labov, Ash, & Boberg, 2005). It is conceivable that these asymmetries are grounded in phonetic differences between laterals and rhotics; however, this possibility is difficult to assess given the information available from previous studies.

To the best of our knowledge, lateral and rhotic production has not yet been systematically compared in the same speakers, in the full range of vowel contexts and syllable positions of General American English. In particular, we lack comprehensive instrumental data on how coda liquids are produced after different vowels, allowing a direct comparison of lateral and rhotic behavior in rimes. Data on liquid production have also been limited in the scope of coverage provided by some sensing modalities. EPG, EMA, XRMB and ultrasound have provided rich data on lingual targets and timing, but each from restricted regions of the tongue. Static structural MRI has facilitated a more complete view of the upper airway and lingual postures associated with liquid allophones, but has not allowed dynamic characterization of vowel-consonant and consonant-vowel coproduction patterns. We address this deficit in this study by making use of the richer information afforded by real-time magnetic resonance imaging (rtMRI: Narayanan, Nayak, Lee, Sethy, & Byrd, 2004) about the dynamic configuration of the vocal tract.

Despite the foregoing deficit in research on liquid production in General American English, previous studies of these consonants in English varieties have yielded an extensive body of work with relevant insights on which we build (in overview, see, e.g., (Gick, 2003; Gick & Campbell, 2003; Krakow, 1999; Proctor & Walker, 2012)). Two key articulatory properties that

* Corresponding author at: Australian Hearing Hub, 16 University Avenue, Macquarie University, NSW 2109, Australia.
*E-mail address:* michael.proctor@mq.edu.au (M. Proctor).

https://doi.org/10.1016/j.wocn.2019.100921
0095-4470/

are common to American English liquids emerge from these studies. The first is *gestural complexity*. Laterals require temporal and spatial coordination of two gestures, which may be loosely characterized as coronal and dorsal (Giles & Moll, 1975; Sproat & Fujimura, 1993), while rhotics are prototypically produced with three coordinated gestures: labial, anterior lingual, and pharyngeal. The second key property is *syllabic positional sensitivity*. Both laterals and rhotics exhibit allophonic variation conditioned by their position in the syllable: post-vocalic laterals are typically 'darker' (produced with a more retracted/lowered tongue body) than their pre-vocalic counterparts (Lee-Kim, Davidson, & Hwang, 2013; Narayanan, Alwan, & Haker, 1997); pre-vocalic /ɹ/ is more labialized and more often retroflexed than its post-vocalic and syllabic variants (Delattre & Freeman, 1968; Mielke, Baker, & Archangeli, 2016; Uldall, 1958; Zawadzki & Kuehn, 1980). Gestural coordination patterns also differ systematically across these environments for both liquids (Browman & Goldstein, 1995a; Gick, Campbell, Oh, & Tamburri-Watt, 2006; Gick, Iskarous, Whalen, & Goldstein, 2003; Scobbie & Pouplier, 2010; Sproat & Fujimura, 1993). Most relevant to our focus on distributions in rimes of General American English is the finding that in coda liquids the more posterior lingual gesture begins before the anterior lingual gesture.

The coupled oscillator model of Articulatory Phonology has been influential in modeling the representation of multi-gestural liquids with regard to coordination of their articulations within and across segments (etc. Browman & Goldstein, 1986, 1989, 1992; Krakow, 1999; Nam, Goldstein, & Saltzman, 2009; Saltzman, Rubin, Goldstein, & Browman, 1987). This is especially important for coda liquids, where the dorsal or pharyngeal gesture precedes a coronal articulation, and therefore potentially shows greater overlap and interaction with the preceding vowel. An examination of coarticulatory effects can shed light on the nature of the interaction between overlapping and competing articulations. Recasens, Pallarès, and Fontdevila (1997) and Recasens and Rodríguez (2016, 2017) have found that the coarticulatory dominance of a segment, referring jointly to its resistance to coarticulation from other segments and the aggressiveness of its coarticulatory effect on other segments, depends on a segment's manner and the articulators involved in its formation. For liquid consonants in Catalan, the trill [r] is found to have a higher coarticulatory dominance than the lateral [l] and the flap [ɾ] (Recasens & Rodríguez, 2016). Bladon and Al Bamerni (1976) found that dark [ɫ] exhibits greater coarticulation resistance (a term they coined) than clear [l] in RP English; however, the relative coarticulatory dominance of the lateral and rhotic in American English have not previously been examined.

In the dynamical formal framework of Articulatory Phonology, differences in coarticulatory dominance can be represented by the specified blending strength for a gesture (Fowler & Saltzman, 1993; Saltzman & Munhall, 1989). In this model, when overlap occurs between two gestures that impose conflicting demands on the same articulator, their goal articulatory states are blended, with the outcome being the weighted average of the individual goal articulatory states, based on the specified blending strength of each. Gestures with a higher specified blending strength are expected to exhibit greater coarticulatory dominance, with the potential to induce stronger neutralization effects on other gestures with which they overlap and to show greater resistance to neutralization. Given that greater neutralization of vowel contrasts occurs before coda rhotics than coda laterals in General American English, we hypothesize that the rhotic has a posterior lingual gesture with stronger blending strength than that of the lateral in this dialect. This hypothesis predicts that the rhotic will show less variance in articulation than the lateral across vocalic contexts and syllable positions, owing to the rhotic's hypothesized greater coarticulatory resistance. It also predicts that the articulation of vowels will be more affected in the context of a coda rhotic than a coda lateral, owing to the rhotic's hypothesized greater coarticulatory aggression.

### *1.1. Goals*

In summary, the goal of this study is to examine in new detail the articulation of liquid-final rimes in General American English, to shed more light on their shared characteristics and the phonotactic asymmetries between liquids and preceding vowels. By making use of the richer information about the configuration of the vocal tract provided by rtMRI, we aim in particular to examine the relative coarticulatory dominance of rhotics and laterals on the following points:

1. compare the articulation of liquid consonants across a complete range of vowel contexts
2. compare the articulation of liquid consonants in coda position with their onset equivalents
3. compare the articulation of vowels produced before coda liquids with vowels unaffected by coarticulatory influences from adjacent liquid consonants

## **2. Material and methods**

We examined patterns of liquid consonant production and coarticulation in the midsagittal plane, using real-time structural magnetic resonance imaging sequences specially developed to track dynamic configuration of the upper airway during speech (Narayanan et al., 2004). This technology offers new insights into liquid consonant production because it images the whole vocal tract, including the tongue body, tongue root and pharynx: regions which have proven difficult to track using other methods, but which provide critical detail about tongue shaping in laterals, rhotics, and vowels, and the coordination of lingual and other gestures.

### *2.1. Subjects and stimuli*

Four native speakers of General American English participated in the study, with ages ranging from 23 to 28 years (Table 1). Although from geographically diverse backgrounds, all four informants are college-educated L1 speakers raised in the USA who were selected for participation because their accents are not characteristic of any particular region, and because both parents are fluent speakers of American English. None of the speakers reported abnormal hearing or speaking development or pathologies.

### *2.2. Experimental materials*

Lateral and rhotic approximants were elicited in onset and coda positions in monosyllabic real and nonce words, adjacent

**Table 1**
Study participants – demographic details

| ID | Gender | Age | Birthplace |
|---|---|---|---|
| W1 | Female | 27 | San Clemente, CA |
| W2 | Female | 27 | Babylon, NY |
| W3 | Female | 28 | Brawley, CA |
| M1 | Male | 23 | Baltimore, MD |

**Table 2**
Experimental materials: elicitation items.

| Context | Onset | | Coda | | Vowel |
|---|---|---|---|---|---|
| | #l | #ɹ | l# | ɹ# | |
| /i/ | leap | reap | peel | beer | beep |
| /ɪ/ | lip | rip | pill | | bib |
| /eɪ/ | lame | rave | bail | bare | babe |
| /ɛ/ | Lev | rep | bell | | pep |
| /æ/ | lap | rap | pal | | bam |
| /ʌ/ | love | rum | mull | | pub |
| /ɑ/ | lob | rob | ball | bar | bob |
| /oʊ/ | lobe | robe | pole | bore | foam |
| /u/ | loop | rube[1] | pool | boor[2] | boom |
| /ʊ/ | loof | | pull | | boof |

[1] Although [ʊ] is attested after [ɹ] in *'rook'* [ɹʊk] in General American English, the [u/ʊ] contrast is neutralized after [ɹ] before a labial coda, with some variability in realization of the vowel. For instance, some speakers pronounce *'room'* as [ɹum] and others as [ɹʊm] (Wells, 2008).

[2] Three of our subjects reported a full or partial merger of back round vowels to [ɔ] before a coda rhotic. Nevertheless, they attempted to produce *'boor'* with a high back vowel.

to each of the vowels of General American English, subject to phonotactic gaps (Table 2). Each vowel-liquid pairing was elicited adjacent to a labial onset or coda consonant, to minimize coarticulatory effects on the target nucleus. In some cases, it is not clear exactly which segment best represents the vowel before a rhotic-final coda, and some contrasts may be partially or fully neutralized for some speakers. In particular, /eɪ/ may be monophthongal [e] in pre-lateral and pre-rhotic contexts, and /oʊ/ may be realized as [oʊ], [o], or [ɔ], depending on speaker and context. Bearing all these factors in mind, the experimental materials were designed to elicit all potentially contrastive liquid-final rimes of General American English.

In addition to these vowel-liquid and liquid-vowel sequences, all vowels were elicited in monosyllabic words with labial onsets and codas (Table 2, last column) to capture intrinsic vowel targets in lexical items with minimal lingual coarticulatory influence from surrounding consonants. Laterals ('*lime*', '*pile*', '*Lao*', '*fowl*', '*lerm*', '*pearl*') and rhotics ('*rhyme*', '*fire*', '*Rao*', '*bour*', '*fur*') were also produced adjacent to the diphthongs /aɪ/ ('*vibe*') and /aʊ/ ('*pow*') and the rhoticized vowel /ɝ/ ('*verb*'), to capture the full range of phonotactic environments in which both liquids may appear in General American English. These data were examined qualitatively, but were not included in the quantitative analyses because they were not directly comparable with liquids produced adjacent to the other vowels: nuclear targets were temporally complex, produced inconsistently across speakers, and/or indistinguishable from rhotic-initial codas.

Five repetitions were elicited for each word with a liquid target, and two repetitions of each vowel target item. Words were presented in pseudo-randomized order, in blocks containing up to 13 items. Nonce words whose vocalic pronunciation was not obvious from their spelling were reviewed in advance with the subjects for their intended pronunciation, and were elicited along with a rhyming word as a reminder, (e.g. *'woof'* for *'boof'*). In addition to the core experimental corpus, four short read passages and some spontaneous speech was elicited from each participant, in recording sessions lasting up to 70 min.

### 2.3. Image and audio acquisition

MRI data were acquired at Los Angeles County Hospital on a Signa Excite HD 1.5T scanner, using a custom upper airway receiver coil array. Each subject's upper airway was imaged while they lay supine in the MRI scanner with their head immobilized. Elicitation items were presented one word at a time, in large text on a back-projection screen which subjects could read from within the scanner bore. Participants adopted similar oral resting postures between utterances: lips closed (W2, W3, M1) or slightly open (W1), tongue tip resting on (W2, W3, M1) or just below (W1) the alveolar ridge, and tongue body resting on (W2) or just below (W1, W3, M1) the hard palate. Rest postures were consistently maintained by each participant throughout the experiment, suggesting that there were no major effects of articulatory setting on patterns of production within or across subjects.

A gradient echo pulse sequence (13 interleaved spiral readout; max. gradient = 4.0 G/cm; max. slew rate = 15.0 G/cm/ms; TR = 6.164 ms) was used to acquire a 5 mm midsagittal slice with image resolution $68 \times 68$ pixels over a $200 \times 200$ mm field of view. Image data were reconstructed as 23.2 frames per second video sequences (Bresch, Kim, Nayak, Byrd, & Narayanan, 2008). Audio was simultaneously recorded at a sampling frequency of 20 kHz inside the MRI scanner while subjects were imaged, using a custom fiber-optic microphone noise-canceling system (Bresch, Nielsen, Nayak, & Narayanan, 2006).

### 2.4. Articulatory analysis

MRI data and companion audio were loaded into a custom graphical user interface for inspection and analysis (Narayanan et al., 2014; Proctor, Bone, & Narayanan, 2010). For each token in the corpus, the interval of image frames containing the utterance was first located using acoustic landmarks. Frame numbers corresponding to articulatory targets were then identified in the MRI video using the following criteria:

- *lateral coronal target*: first frame after completion of tongue tip (TT) constriction, or maximum advancement of TT within acoustic interval of utterance when no coronal constriction is achieved
- *lateral dorsal target*: maximum tongue body (TB) retraction during lateral production interval
- *rhotic labial target*: maximum labial (LAB) compression/protrusion during rhotic production interval
- *rhotic dorsal target*: maximum TB retraction/lowering during rhotic production interval
- *rhotic coronal target*: closest approximation of front of tongue to palate during rhotic production interval
- *vowel target posture*: center frame of most stable interval associated with primary vocalic goal (corresponding to monophthongal vowel target after any on-glide, or first target of diphthongs)

Landmarks were identified by manual inspection of the speech interval of interest, reviewing the video sequences frame-by-frame, forward and reverse, until the video frame which optimally satisfied the selection criteria was located. Coronal and labial landmarks were identified as the frame in which pixel brightness was maximized in the region of the target constriction, since mean pixel intensity is correlated with the amount of soft tissue in a region in rtMRI (Proctor et al., 2011). Landmark analysis was performed with reference to the entire tip and body of the tongue – making use of the global view of lingual configuration provided by rtMRI – rather than tracking specific flesh-points on these articulators, as in EMA analysis.

*Tissue boundary location*. Reference vocal tract outlines were located for each speaker in the palate and pharynx using mean image sets, and superimposed on each image frame to define passive tract boundaries. Midsagittal tongue and lip outlines were then located in each MRI frame in the sequences of interest (Fig. 1), using a tissue tracking algorithm operating over intensity profiles constrained by a semi-polar analysis grid (details in Proctor et al., 2010).

*Tracking change in midsagittal articulation*. Sequences of tongue edges were extracted from the temporal intervals demarcated by the landmarks defined in Section 2.4. These image sequences show change in lingual posture from coronal consonant targets to vowel target for onsets, and from vowel to coronal consonant targets for coda liquids (Fig. 2). At each articulatory landmark of interest, tongue edges were extracted from each token so that mean tongue postures could be calculated and compared. Tongue postures were extracted from the second, third and fourth repetitions of each word. The first repetition, produced while the participants adjusted to the task of reading prompted speech in a noisy MRI scanner, was excluded from the analysis in case these utterances were atypical or erroneous; the fifth repetition was used in cases where one of the previous tokens was mispronounced, so that three tokens were analyzed for each vowel-liquid and liquid-vowel sequence.

*Mean articulatory targets*. Characteristic midsagittal lingual postures associated with segments of interest were derived by calculating mean tongue positions at equivalent points in time across multiple tokens. Average target tongue shapes of rhotics and laterals produced by each speaker were generated by calculating the Euclidean mean point on each analysis gridline, from the set of all exemplars of each consonant. Mean lingual outlines were calculated from 33 tokens of each speaker's onset rhotic (3 repetitions $\times$ 11 vowel contexts), 39 tokens of each onset lateral (3 $\times$ 13 vowel contexts), 24 tokens of each speaker's coda rhotic (3 $\times$ 8 vowel contexts), and 39 tokens of each coda lateral (3 $\times$ 13 vowel contexts).

*Coarticulatory influence*. The coarticulatory influence of liquid consonants on tautosyllabic vowels was estimated by comparing mean tongue posture at vowel target in liquid-initial and liquid-final words[1] with the shape of the tongue captured during separate production of the same vowel in an inter-labial context (Table 2, rightmost column). The Euclidean distance between the two mean tongue edges was calculated along each analysis gridline over the length of the tongue, from the sublingual cavity to the tongue root (Fig. 3). Total lingual displacement from intrinsic vocalic posture was calculated as the sum of all distances (mm) between the two mean tongue postures: the higher the sum of distances, the greater the total displacement of the lingual shape in a vowel, attributable to the coarticulatory influence, or 'aggressiveness' (Farnetani, 1990; Fowler & Saltzman, 1993; Recasens & Espinosa, 2009), of the adjacent consonant.

*Coarticulatory resistance*. Coarticulatory resistance (Bladon & Al Bamerni, 1976; Recasens, 1984) of liquid consonants was estimated by examining variability in tongue shaping across a set of liquid tokens produced in different vocalic contexts. Consonants produced before and after the common set of vowels /ɪ-ɛ-ɑ-oʊ-ʊ/ were captured at the dorsal target frame, and mean tongue postures were calculated from all repetitions of the same liquid in the same syllable context. The Euclidean distance between each tongue edge and the mean posture was calculated at each point along the subset of gridlines extending from the midsagittal cavity to the tongue root-epiglottal junction. Variance of displacement from mean tongue posture was also calculated at each gridline for each set of tongue edges representing the same liquid allophone (Fig. 4). Mean total displacement and mean total variance (averages of group means and variances calculated at each grid line) were calculated to estimate coarticulatory resistance across the common set of context vowels.

### 2.5. Statistical analysis

Because of the small number of participants, and consistent with the goals of the study, details of individual liquid production are reported, along with statistical analyses of the major patterns of production identified across all speakers. Statistical analysis was conducted in R version 3.5.1 (R Core Team, 2018). Linear mixed effects models were fitted with the *lme4* package (Bates, Mächler, Bolker, & Walker, 2015) using restricted maximum likelihood (REML). The optimal model for each analysis was determined to be the one with the lowest Akaike Information Criterion (AIC) among candidate models refitted using maximum likelihood (ML) to maximize goodness-of-fit. Individual speaker differences were modelled using random intercepts for Subject unless models with by-speaker random slopes for fixed effects provided a significantly better fit ($\chi^2$ tests, $p < 0.05$). Simpler models were also used when fitted vs. residual plots of extended models revealed large deviations from linearity or when residual quantile-quantile plots revealed large deviations from normality, and when models failed to converge due to data sparsity or imbalance. $t$-statistics, $F$-statistics, and corresponding $p$-values were calculated with the *lmerTest* package (Kuznetsova, Brockhoff, & Christensen, 2017) using Satterthwaite's method for denominator degrees of freedom.

Standardized effect sizes and power analyses are also reported to facilitate interpretation of the results with respect to the scope of the study (Kirby & Sonderegger, 2018). Standardized effect sizes ($d$) were calculated with variance components (Brysbaert & Stevens, 2018), using the method for fully-crossed designs in mixed effects models described in Westfall, Kenny, and Judd (2014). Power estimates were conducted with Monte Carlo simulations, using the *simr* package (Green & MacLeod, 2016). Power calculations were made over

[1] What the intrinsic vowel target is before a rhotic deserves consideration. We return to this issue in Section 3.6.

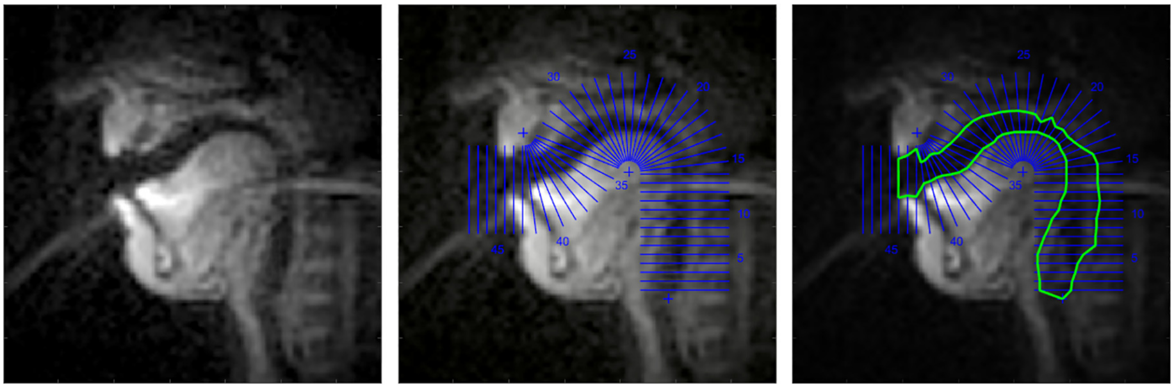

**Fig. 1.** Midsagittal tissue boundary segmentation in rtMRI data. Left: Image frame captured at articulatory target of low front vowel after onset lateral (Subject M1: *'lap'*). Centre: Semi-polar vocal tract analysis grid (blue radial lines) superimposed on image; Right: tissue boundaries (green outline) located from pixel intensity thresholds. Arc-shaped artifact passing through lower lip, tongue body and pharynx caused by co-planar cardiac activity. (For interpretation of the references to colour in this figure legend, the reader is referred to the web version of this article.)

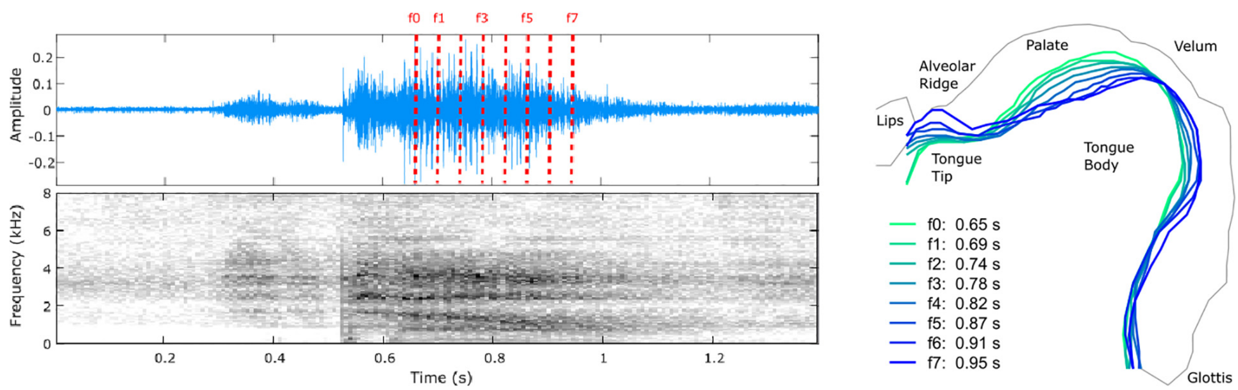


**Fig. 2.** Tracking change in midsagittal lingual posture. Left: speech waveform (top) and spectrogram (bottom) of lateral-final utterance (Subject M1: *'pal'*). Right: tongue edges captured at 43 ms intervals, from nuclear vowel target (green) to coda posture at lateral coronal target (blue). Broken (red) lines superimposed on waveform show points in time and image frame numbers from which each tongue edge is captured in articulatory sequence. Spectrogram shows broadband background noise characteristic of in-scanner speech recordings. (For interpretation of the references to colour in this figure legend, the reader is referred to the web version of this article.)

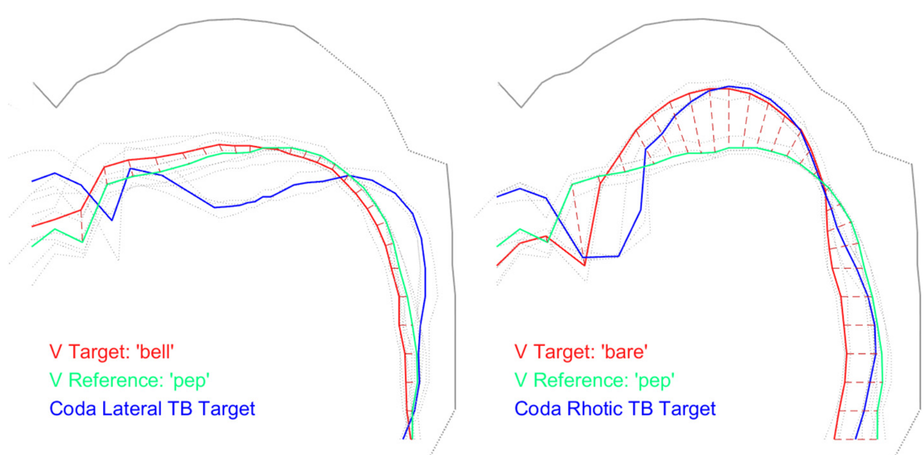


**Fig. 3.** Quantifying consonant-vowel coarticulation. Green tongue outline: intrinsic posture of vowel [ɛ] in inter-labial context ('*pep*'), where coarticulatory influences are minimal. Solid red lines: mean lingual postures of same vowel produced adjacent to liquid consonants. Blue lines: mean tongue posture at dorsal target of tautosyllabic liquid. Lingual displacement due to coarticulatory influence of consonant is calculated as total Euclidean distance between vowel postures along all analysis gridlines intersecting the tongue between sublingual cavity and tongue root (broken red connecting lines). Left: [ɛ] before coda lateral ('*bell*'); Right: [ɛ] before coda rhotic ('*bare*'). (All comparisons: Speaker W1.) (For interpretation of the references to colour in this figure legend, the reader is referred to the web version of this article.)

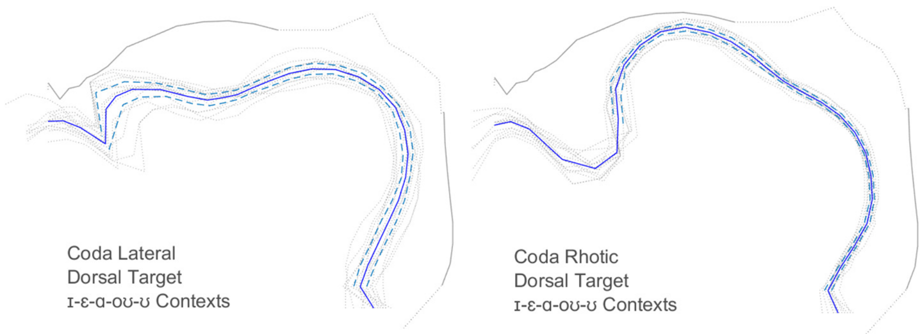


**Fig. 4.** Quantifying coarticulatory resistance. Variance in displacement from mean posture of coda liquids following vowels /ɪ-ɛ-ɑ-oʊ̆-ʊ̆/. Left: coda lateral; Right: coda rhotic (Speaker W2). Light grey lines: tongue posture at dorsal target in each liquid token. Blue solid lines: mean tongue posture across all tokens. Blue dashed lines delimit two standard deviations of displacement from mean tongue posture: greater separation indicates greater variance in tongue shape at consonantal target due to coarticulatory effects of adjacent vowel. (For interpretation of the references to colour in this figure legend, the reader is referred to the web version of this article.)

1,000 simulations at a significance level of $\alpha = 0.05$, using Type-II tests with Satterthwaite denominator degrees of freedom.

## 3. Results

We first describe the articulatory characteristics of each liquid as revealed by rtMRI: the gestures associated with each consonant at each syllable margin, and the ways that they differ between speakers and allophones. Gestural characterization of each liquid establishes a set of common landmarks for reference in the analysis of coarticulation, and provides a validation of these data in broad strokes against what is known from previous studies about the articulation of liquids. To illustrate the tongue postures characteristic of each liquid at each syllable margin, laterals and rhotics produced in a low vowel context by Speaker M1 are juxtaposed in Fig. 5.

### *3.1. Articulatory characterization of lateral allophones*

Mean tongue postures for word-initial laterals are contrasted with mean coda lateral postures in Fig. 6. Onset laterals were produced with an apical coronal closure against the back of the upper incisors (Fig. 5, left panel), accompanied by retraction of the tongue body towards a uvular (W2, W3, M1) or pharyngeal (W1) target (Fig. 6). Coda laterals were produced with the same two gestures; however, complete constriction of the tongue-tip against the teeth or alveolar ridge was achieved much less consistently than in initial allophones. All coda laterals of W3 and M1 concluded with full TT closure, but none of the 30 word-final laterals were produced by W1 with full tongue-tip closure. In 13% of W2's final laterals, coronal closure was not achieved before the acoustic end of the utterance. In the most vocalized coda lateral realizations (those with the greatest degree of lenition of the anterior gesture in the midsagittal plane: Fig. 6, left panel), the tongue tip approached no closer to the alveo-dental target than 10 mm (W1 '*pal*') and 8 mm (W1 '*pool*').

Individual speakers differ in the positioning of the tongue body in lateral production: M1, W2 and W3 retract the rear of the tongue towards the uvula, consistent with previous descriptions of American English /l/ (Bladon & Al Bamerni, 1976; Giles & Moll, 1975), while the posterior gesture of W1's lateral is lower and post-uvular, and better characterized as having a mid-pharyngeal target, even in onset position (Fig. 6, left panel). The minimal constriction between the back of the tongue and the rear pharyngeal wall/uvula was located 65 mm above the glottis for M1, and 27 mm above the glottis in mean coda posture for W1.

The rearmost part of the tongue body was, on average, more retracted in word-final laterals produced by all speakers (Fig. 6). The grand mean difference in TB retraction between onset and coda laterals (all speakers, all tokens) was $-2$ mm. Mean minimum pharyngeal aperture was 2 mm more constricted in coda laterals, compared to onsets. For all speakers, the front of the dorsum is lower in coda [ɫ], compared to the onset lateral: the height difference – measured at the point of greatest difference between mean lateral postures posterior to the tongue blade – varied from 6 mm (M1) to 10 mm (W1); the mean greatest difference in dorsal tongue height between onset and coda laterals across all speakers was 7 mm. W1 also showed the greatest difference in coronal articulation between positional allophones: her coda laterals were produced without complete tongue tip closure in the midsagittal plane, and her mean coda lateral posture is highly vocalized, displaying a large aperture (14 mm) between the closest point of excursion of the tongue tip to the alveolar ridge (Fig. 6, left panel).

### *3.2. Articulatory characterization of rhotic allophones*

Mean midsagittal tongue postures for rhotic approximants produced in syllable onset position are compared with mean postures for coda rhotics[2] in Fig. 7. Three gestures could be identified in word-initial rhotics produced by all speakers: labial approximation, coronal approximation towards the palate, and tongue root retraction/lowering (e.g. Fig. 5, 3rd panel). Labial approximation – sometimes accompanied by lip protrusion – was clearly observed in all 108 onset rhotics analyzed (27 tokens $\times$ 4 speakers), as was the onset rhotic coronal gesture. Retraction of the tongue body towards the lower rear pharyngeal wall was observed in all word-initial rhotics, accompanied by a tongue root lowering gesture at the base of the epiglottis, towards the glottis. Although the dorsal retraction associated

[2] Some details of the geometry of sublingual cavities may appear simplified in figures illustrating mean tongue outlines, as a result of averaging of air-tissue boundaries across analysis gridlines spaced up to 5 mm apart.

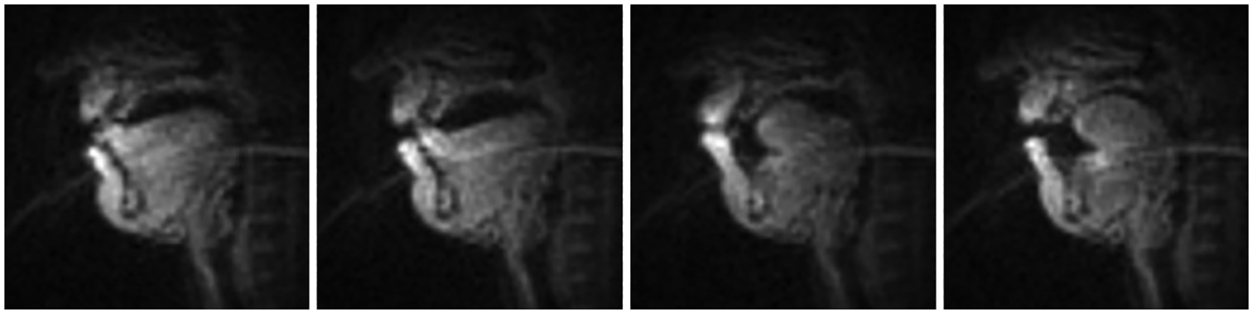

**Fig. 5.** Illustrative liquid postures: low vowel context, subject M1. Left-to-right: Onset lateral ‘*lob*’, coda lateral ‘*ball*’, onset rhotic ‘*rob*’, coda rhotic‘*bar*’. Tongue captured at coronal target of each liquid.

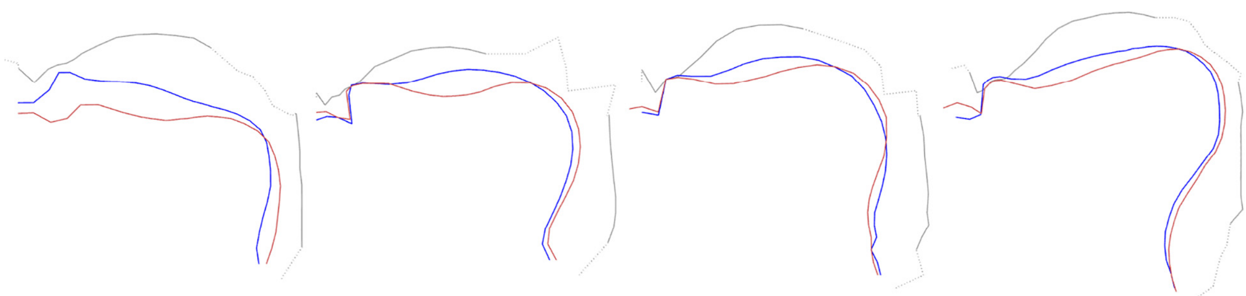

**Fig. 6.** Mean lateral articulatory postures: onsets vs. codas, all vowel contexts. Blue lines: mean midsagittal tongue shape at onset coronal target (all lateral-initial tokens); Red lines: mean midsagittal tongue shape at coda coronal target (all lateral-final tokens); Left-to-right: Subjects W1, W2, W3, M1. Grey lines depict palatal and pharyngeal outlines. Broken grey lines show indicative posture of (variably articulated) soft palate and lower pharynx. (For interpretation of the references to colour in this figure legend, the reader is referred to the web version of this article.)

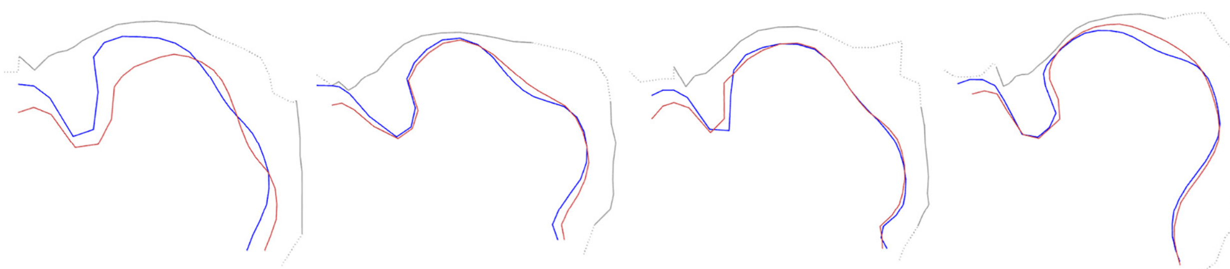

**Fig. 7.** Mean rhotic articulatory postures: onsets vs. codas, all vowel contexts. Blue lines: mean midsagittal tongue shape at onset coronal target (all rhotic-initial tokens); Red lines: mean midsagittal tongue shape at coda coronal target (all rhotic-final tokens); Left-to-right: Subjects W1, W2, W3, M1. Grey lines depict palatal and pharyngeal outlines. (For interpretation of the references to colour in this figure legend, the reader is referred to the web version of this article.)

with rhotic production was not always distinguishable from the tautosyllabic vowel gesture, some lowering of the tongue root was identifiable in onset rhotics produced before all vowels.

Coda rhotics were characterized by a dorsal gesture produced before, or at the same time as, approximation of the front of the tongue towards the palate (Figs. 9, 11, 13, 15, bottom rows). There was no evidence of a labial gesture in coda rhotics produced by speakers W1, W3, and M1 (Fig. 5, right panel); even in words containing a rounded vowel (‘*bore*’, ‘*boor*’, ‘*bour*’), the lips invariably moved apart in the transition from the nucleus to the rhotic coda. Some lip protrusion accompanied the coda rhotic in two utterances of ‘*beer*’ by W2, but as with the other speakers, no labial approximation was observed in word-final rhotics produced by W2 after any vowel.

Individual speakers’ rhotics vary in how bunched the tongue is, and in the degree and location of the oral constrictions (Fig. 7). Coronal constrictions range in anteriority, with part of the tongue approaching a post-alveolar target in the most advanced realizations (M1), but all speakers’ rhotics are articulated with a large mass of the front part of the tongue approximating the hard palate. The minimum mean aperture of the coronal constriction ranges from 1 mm (M1 onset and coda) to 14 mm (W1 coda). The most constricted part of the posterior oral cavity is located low in the pharynx for Speaker W1 (13 mm above the glottis in mean coda posture), in the upper pharyngeal region for M1 (58 mm above the glottis in mean onset posture), and at mid-pharyngeal positions for W2 and W3 (mean 30 mm above glottis).

Despite these individual differences, the word-initial rhotics produced by all four speakers are characterized by five shared midsagittal articulatory properties: (i) bilabial approximation; (ii) a prominent sub-lingual cavity; (iii) approximation of a broad part of the front of the tongue towards the post-alveolar/

palatal region; (iv) a pharyngeal constriction; and (v) a region of concave curvature in the middle of the tongue (a mid-dorsal saddle). Midsagittal tongue shapes of coda rhotics closely resemble those produced in syllable onset position by the same speakers. The most pronounced difference between the two mean postures is the absence of labialization in coda /ɹ/. Linear mixed models with random intercepts for subject were constructed to test the effects of syllable position (onset/-coda) on labial posture on rhotics (measured at the coronal target frame). Labial aperture is more constricted in onsets ($\beta = -9.2$ mm, $t(163) = -18.8$, $p < 0.001$; $d = -1.97$, POWER = 100%), and lips are more protruded in onset rhotics ($\beta = 5.7$ mm, $t(163) = 11.72$, $p < 0.001$; $d = 1.20$, POWER = 100%), compared to coda allophones (Details of statistical models in A).

### 3.3. Gestural coordination in liquids

Mean inter-gestural timing relationships for laterals produced by each speaker are summarized in Table 3; mean gestural lags for rhotics are given in Table 4. For each speaker, mean time of achievement of tongue tip and tongue body gestures are calculated relative to the articulatory target of the nuclear vowel ($t = 0$) in each token. For onset rhotics, mean time of maximum labial approximation is also reported. Because the rtMRI data are acquired at 23.2 f.p.s., timing differences smaller than 43 ms cannot be resolved without interpolation, and mean lag calculations are clustered around integral multiples of this minimum timeslice (86 ms = 2 frames; 129 ms = 3 frames; etc.). Despite these limitations, these data reveal clear intergestural timing patterns and ordering relationships associated with the allophones of each liquid.

In onset position, lateral production invariably commences with tongue-tip closure, achieved approximately 90 ms before the tongue body reaches its point of maximum retraction. The post-lateral vowel reaches its articulatory target approximately 190 ms after the dorsal gesture. Coda laterals are realized with the reverse temporal sequencing of gestures: maximum dorsal retraction is achieved approximately 200 ms after the vowel reaches its gestural target, followed 150 ms later (grand mean) by coronal closure or maximum tongue tip advancement.

Onset rhotic production is initiated with labial approximation, which reaches its target – a narrow labial constriction typically accompanied by some protrusion – immediately prior to, or at the same time that the two lingual gestures reach their targets. On average, the labial gesture precedes the lingual gestural targets by 20 ms (grand mean). In all onset rhotics, tongue tip and tongue body/root gestures reached their respective targets within the same frame, approximately 200 ms before the vowel gesture. Word-final rhotics are not characterized by the same synchrony of lingual gestures. In three utterances of '*beer*' by M1, the dorsal and coronal gestures reach their targets in the same frame, but in all other coda rhotics, the posterior gesture precedes the anterior gesture. On average, the TB target is achieved 220 ms after the vocalic target, followed 80 ms later by the coronal gesture.

Linear mixed models with random intercepts for subject were constructed to test the effects of consonant type on the relative timing of lingual gestures at each syllable margin. All timings are expressed with respect to the nucleus, so that gestures achieved before the vowel target (V) have a negative lag, and coda gestures have a positive lag. Consonant type was treatment coded (LATERAL = 0; RHOTIC = 1) so that model intercepts correspond to lag estimates for laterals, and beta coefficients represent the effect of rhotics on lag. In onsets, TT-V lag is shorter for rhotics ($\beta = 66$ ms, $t(223) = 9.98$, $p < 0.001$; $d = 1.29$, POWER = 100%), and TB–V lag is longer for rhotics ($\beta = -20$ ms, $t(223) = -3.17$, $p = 0.0018$; $d = -0.41$, POWER = 89.6%) compared to laterals. In codas, V–TT lag is shorter for rhotics ($\beta = -44$ ms, $t(175) = -4.34$, $p < 0.001$; $d = -0.42$, POWER = 99.2%), V–TB is longer for rhotics

**Table 3**
Mean inter-gestural timing for lateral allophones. TT: tongue-tip closure; TB: maximum retraction of tongue body. Mean (s.d.) timings from 30 utterances: three repetitions of each liquid in ten different vocalic contexts (Table 2). All times (ms) calculated w.r.t. frame in which tongue body achieves vowel target (V).

| | ONSET LATERAL | | | CODA LATERAL | | |
|---|---|---|---|---|---|---|
| | TT | TB | V | V | TB | TT |
| W1 | −265 (57) | −181 (60) | 0 | 0 | 253 (72) | 506 (87) |
| W2 | −292 (43) | −198 (39) | 0 | 0 | 165 (67) | 288 (44) |
| W3 | −278 (45) | −187 (43) | 0 | 0 | 144 (77) | 282 (53) |
| M1 | −262 (53) | −183 (48) | 0 | 0 | 219 (85) | 298 (58) |
| Mean: | −274 (50) | −187 (47) | 0 | 0 | 195 (75) | 343 (61) |

**Table 4**
Mean inter-gestural timing for rhotic allophones. LAB: maximum labial approximation; TT: tongue-tip closure; TB: tongue body/root gestural target. Mean (s.d.) onset timings from 27 utterances: three repetitions of each rhotic in nine different vowel contexts. Mean coda timings from 15 utterances: three repetitions of each rhotic after five different vowels (Table 2). All times (ms) calculated w.r.t. frame in which tongue body achieves vowel target (V).

| | ONSET RHOTIC | | | | CODA RHOTIC | | |
|---|---|---|---|---|---|---|---|
| | LAB | TT | TB | V | V | TB | TT |
| W1 | −249 (55) | −219 (59) | −219 (59) | 0 | 0 | 244 (53) | 351 (46) |
| W2 | −248 (47) | −219 (46) | −219 (46) | 0 | 0 | 193 (32) | 285 (43) |
| W3 | −221 (55) | −205 (52) | −205 (49) | 0 | 0 | 193 (32) | 259 (36) |
| M1 | −198 (42) | −187 (41) | −187 (41) | 0 | 0 | 253 (63) | 302 (49) |
| Mean: | −229 (50) | −207 (49) | −207 (49) | 0 | 0 | 221 (45) | 299 (43) |

($\beta$ = 26 ms, $t(175)$ = 2.40, $p$ = 0.018; $d$= 0.32, POWER = 65.1%), and TB–TT is shorter for rhotics ($\beta$ = −70 ms, $t(175)$ = −7.82, $p$ < 0.001; $d$ = 0.88, POWER = 100%) compared to laterals. Details of all statistical analyses are provided in Appendix B. Residual analyses suggest that these models are robust (quantile-quantile and fitted vs. residual plots showed residuals to be broadly normally distributed and homoscedastic), and power analyses indicate that the data are able to robustly discriminate all timing differences except the V–TB lag in codas. Nevertheless, these results should be interpreted with caution, bearing in mind that the temporal resolution of the data is 43 ms.

### 3.4. Patterns of onset and coda liquid coarticulation

Having identified each speaker's characteristic tongue shape at rhotic and lateral targets, we tracked the change in tongue shape over time as liquid consonants were coproduced with different vowels. Image sequences showing the evolution of lingual configuration between vocalic and liquid articulatory landmarks were superimposed using the method illustrated in Fig. 2, to examine specific patterns of coarticulation for rhotics and laterals, and to see how these patterns vary between onsets and codas.

*Liquid articulation in front vowel contexts*. Lateral approximants produced before and after the high front vowel /ɪ/ are compared in Fig. 8. The coarticulatory influence of the following vowel on word-initial laterals can be seen in the blue (consonantal) frames (Fig. 8, top row), where the front of the dorsum (mid region of the tongue beneath the palate) overlaps more closely with the vowel posture (green frames), compared to the lateral-final sequences (Fig. 8, bottom row). The saddle between the front and back of the tongue is more convex for all speakers' [l] in '*pill*', compared to '*lip*'.

For all four speakers, rhotics produced before /ɪ/ show considerable dorsal overlap between consonantal and vocalic postures in the pharyngeal region (Fig. 9, top row). Coda rhotics produced after the same vowel (Fig. 9, bottom row) involve greater displacement of the back of the tongue towards the rear pharyngeal wall in the transition from vowel to coda in '*beer*'. The most notable asymmetry for rhotics produced in this vowel context is the greater overlap of vocalic and consonantal tongue posture in the coronal region for word-final rhotics compared to their word-initial allophones, which are characterized by greater displacement of the front part of the tongue in the transition into the following vowel in '*rip*'.

Laterals and rhotics produced before and after a mid front vowel are compared in Figs. 10 and 11. The same patterns and asymmetries observed in the high front vowel context are also evident here: onset laterals ('*Lev*') show less mid-dorsal displacement from the posture of the tautosyllabic vowel compared to coda laterals ('*bell*'), and little displacement can be seen between consonantal and vocalic postures in the lower pharyngeal region in either syllable context. As in the /ɪ/ context, coda rhotics produced after /ɛ/ ('*bare*') show more tongue root retraction and greater coronal overlap between vocalic and consonantal postures than in onset position ('*rep*'), where greater anterior lingual displacement is observed compared to '*bare*'. Similar patterns of articulation to those illustrated in Figs. 8–11 are also observed for liquids produced in /i/ ('*leap*', '*peel*', '*reap*'), /eɪ/ ('*lame*', '*bail*', '*rave*'), and /æ/ ('*lap*', '*pal*', '*rap*') contexts.

*Liquid articulation in low vowel contexts*. Lateral production in a low vowel context (/ɑ/) is illustrated in Fig. 12. Individual variability can be observed in the height of the dorsum at the vowel target – W2, in particular, shows a higher dorsal posture at the start of the vowel – but all speakers produce this vowel with retraction/lowering of the back of the tongue into the pharynx, and lowering of the whole front of the tongue to create a large cavity under the palate. In comparison to laterals produced adjacent to front vowels, there is much less movement of the back of the tongue, both in the transition from onset [l]

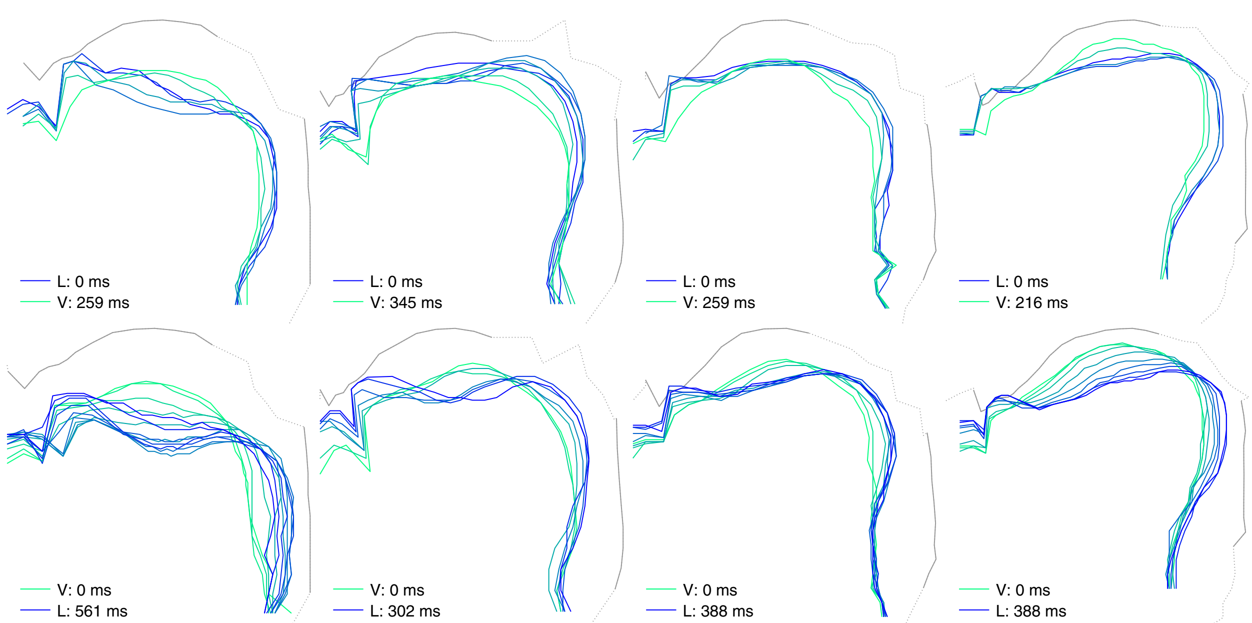


**Fig. 8.** Lateral production in high front vowel context. Top row: onset ('*lip*'); Bottom row: coda ('*pill*'); Left-to-right: Speakers W1, W2, W3, M1; Blue lines: tongue posture at lateral coronal target; Green lines: vowel target posture. Intermediate colors: tongue postures captured at 43 ms intervals in the transition between lateral and vowel. (For interpretation of the references to colour in this figure legend, the reader is referred to the web version of this article.)

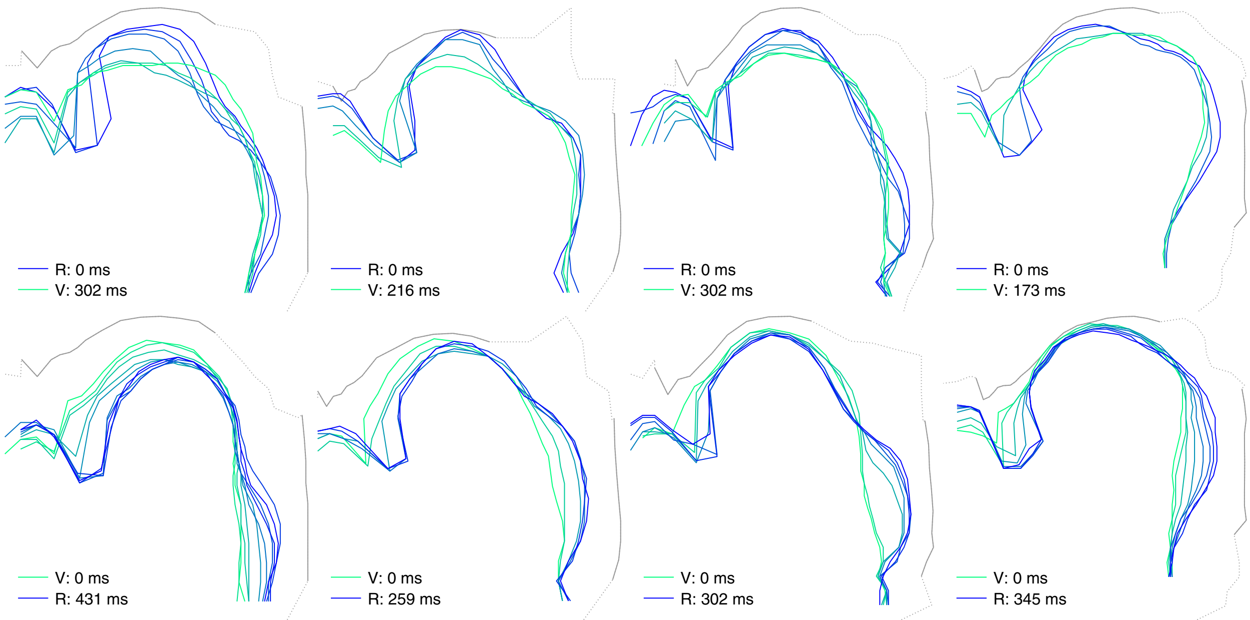


**Fig. 9.** Rhotic Production in High Front Vowel Context. Top row: onset (*'rip'*); Bottom row: coda (*'beer'*); Left-to-right: W1, W2, W3, M1; Blue lines: tongue posture at rhotic coronal target; Green lines: vowel target posture. Intermediate colors: tongue postures captured at 43 ms intervals in the transition between rhotic and vowel. (For interpretation of the references to colour in this figure legend, the reader is referred to the web version of this article.)

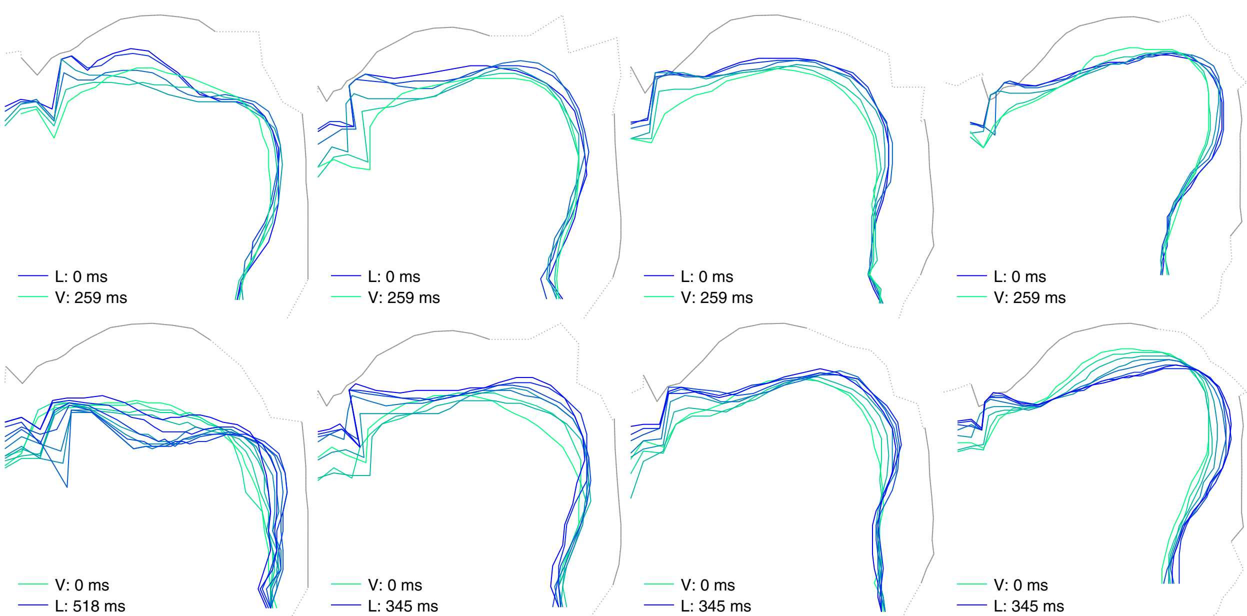


**Fig. 10.** Lateral production in mid front vowel context. Top row: onset (*'Lev'*); Bottom row: coda (*'bell'*); Left-to-right: W1, W2, W3, M1; Blue lines: tongue posture at lateral coronal target; Green lines: vowel target posture. Intermediate colors: tongue postures captured at 43 ms intervals in the transition between lateral and vowel. (For interpretation of the references to colour in this figure legend, the reader is referred to the web version of this article.)

into the vowel ('*lob*'), or from the vowel into the coda lateral ('*ball*'). For speaker M1, the entire back of the tongue – from the root to the blade – remains stationary throughout the [ɑɫ] rime (Fig. 12, bottom right). For all speakers, there is very little displacement of the tongue root and the back of the tongue in the mid-pharyngeal region, either in onset or coda, despite the large amount of the coronal movement, and despite the fact that these sequences begin at the coronal target, which is more peripheral to the nucleus than the dorsal context in all cases (Table 3). This suggests that the intrinsic dorsal target of the lateral is very similar to that of /ɑ/, and/or the lateral dorsal gesture is highly coarticulated with this vowel.

Rhotics produced before and after the low vowel /ɑ/ are compared in Fig. 13. In this vowel context, rhotics produced by all speakers show high stability in the tongue root and tongue back in onset position ('*rob*'), where coronal and dorsal gestures are synchronous or near-synchronous (Table 4). Word-finally ('*bar*'), where the rhotic dorsal gesture precedes

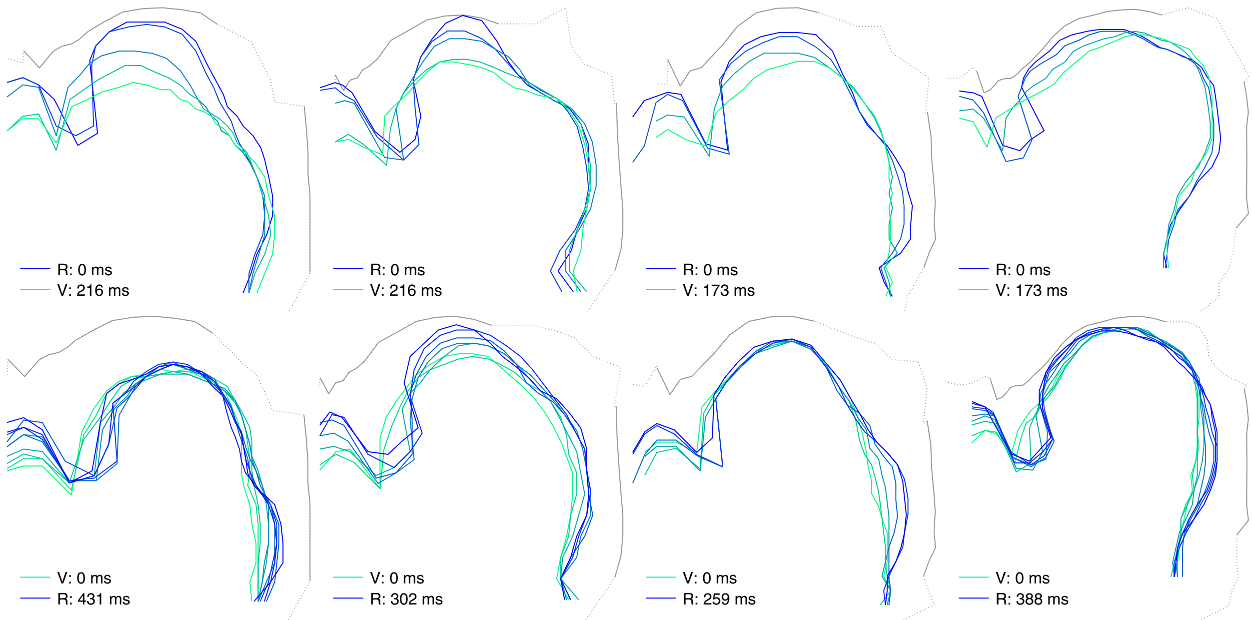


**Fig. 11.** Rhotic production in mid front vowel context. Top row: onset (*'rep'*); Bottom row: coda (*'bare'*); Left-to-right: W1, W2, W3, M1; Blue lines: tongue posture at rhotic coronal target; Green lines: vowel target posture. Intermediate colors: tongue postures captured at 43 ms intervals in the transition between rhotic and vowel. (For interpretation of the references to colour in this figure legend, the reader is referred to the web version of this article.)

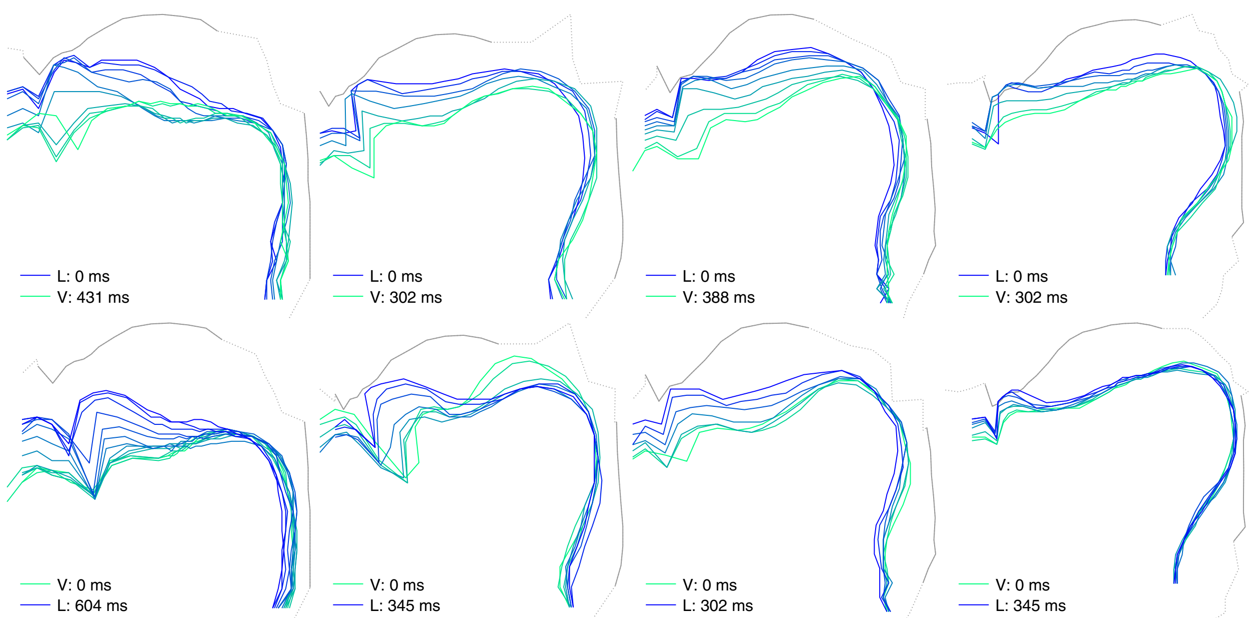


**Fig. 12.** Lateral production in low vowel context. Top row: onset (*'lob'*); Bottom row: coda (*'ball'*); Left-to-right: W1, W2, W3, M1; Blue lines: tongue posture at lateral coronal target; Green lines: vowel target posture. Intermediate colors: tongue postures captured at 43 ms intervals in the transition between lateral and vowel. (For interpretation of the references to colour in this figure legend, the reader is referred to the web version of this article.)

the coronal gesture, more lingual displacement can be seen in the pharynx (Fig. 13, bottom row), in the transition from the nucleus to coda. In both syllable positions, rhotics produced by all speakers in the low vowel context are characterized by large amounts of movement of the entire front part of the tongue towards or from the palatal approximant target. Speaker W3 shows the greatest asymmetry between [-ɑɹ] and [ɹɑ-], which is slightly retroflexed at the coronal target; but all speakers use the same global tongue shape for rhotics produced at both syllable margins. Similar patterns of articulation to those illustrated in Figs. 12 and 13 are also observed for liquids produced in /ʌ/ ('*love*', '*mull*', '*rum*') contexts.

*Liquid articulation in back vowel contexts*. Laterals produced before and after /oʊ/ are compared in Fig. 14. As in the low vowel context, coda laterals produced by all speakers are characterized by high stability across the entire back of the tongue, from the root to the top of the dorsum. For all speakers, the onset in '*lobe*' is less articulatorily similar to [oʊ] than the

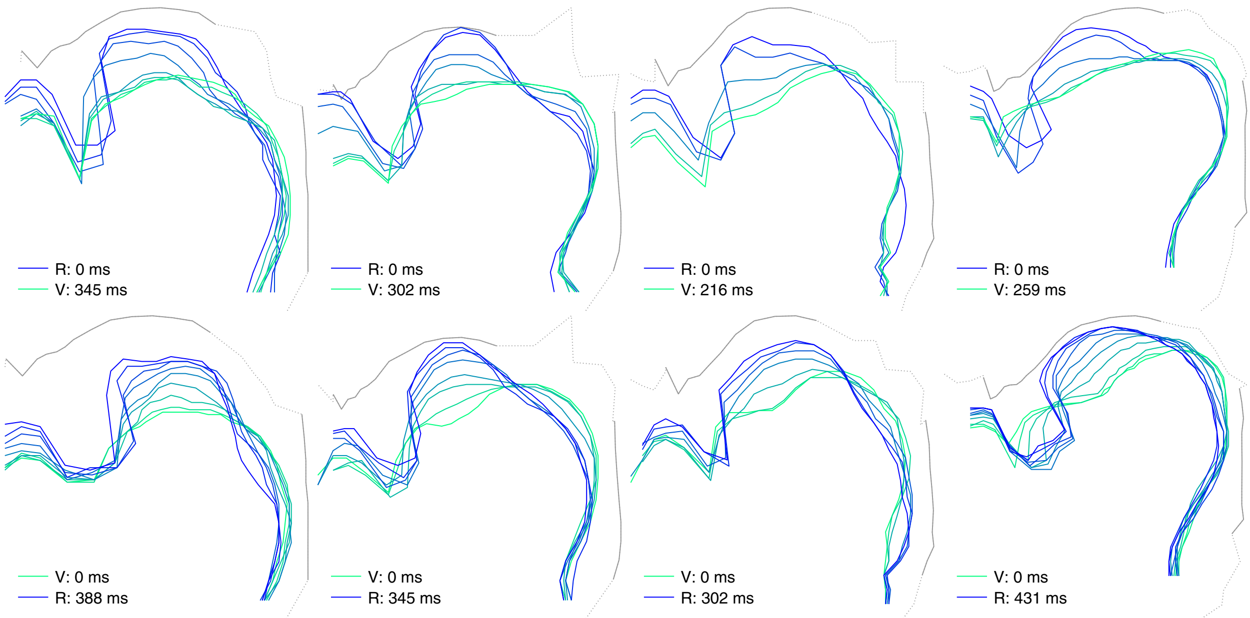


**Fig. 13.** Rhotic production in low vowel context. Top row: onset (*'rob'*); Bottom row: coda (*'bar'*); Left-to-right: W1, W2, W3, M1; Blue lines: tongue posture at rhotic coronal target; Green lines: vowel target posture. Intermediate colors: tongue postures captured at 43 ms intervals in the transition between rhotic and vowel. (For interpretation of the references to colour in this figure legend, the reader is referred to the web version of this article.)

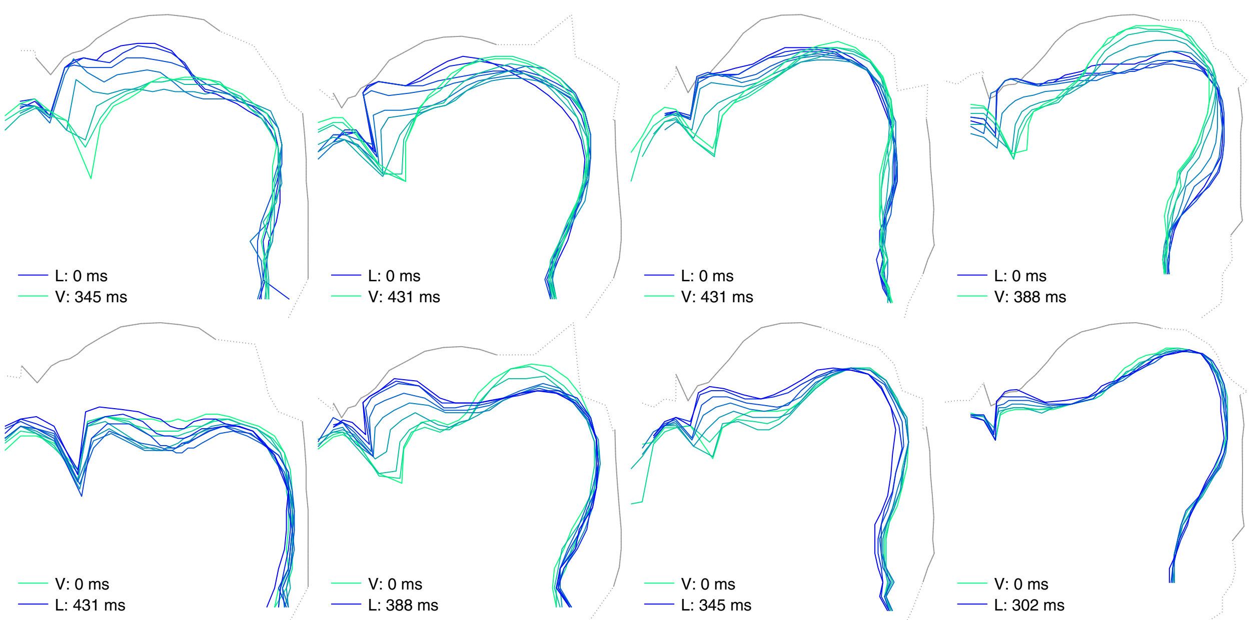


**Fig. 14.** Lateral production in back vowel context. Top row: onset (*'lobe'*); Bottom row: coda (*'pole'*); Left-to-right: W1, W2, W3, M1; Blue lines: tongue posture at lateral coronal target; Green lines: vowel target posture. Intermediate colors: tongue postures captured at 43 ms intervals in the transition between lateral and vowel. (For interpretation of the references to colour in this figure legend, the reader is referred to the web version of this article.)

coda allophones following the same vowel ('*pole*'). As in the low vowel context, onset laterals are produced with the tongue blade and the front of the dorsum raised and less concave than the coda variants in '*pole*'. Onset/coda lateral asymmetries are especially pronounced for M1, who has a high back initial vocalic target for [oʊ] in '*lobe*', requiring raising and backing of the entire tongue body from the mid-pharyngeal target of the initial lateral. In contrast, M1's coda lateral following the same vowel is produced with virtually no movement from the preceding [oʊ] (Fig. 14, bottom right panel), maintaining the same global tongue posture throughout the entire rime of '*pole*'.

Fig. 15 compares rhotics produced before and after the back vowel /oʊ/. Unlike laterals produced in back vowel contexts, all rhotics show displacement of the back of the tongue in the transition to ('*robe*') or from ('*bore*') the vowel target. At both syllable margins, rhotics are produced with a constriction in the lower (W1, W3), mid (W2) or upper (M1) pharynx that dif-

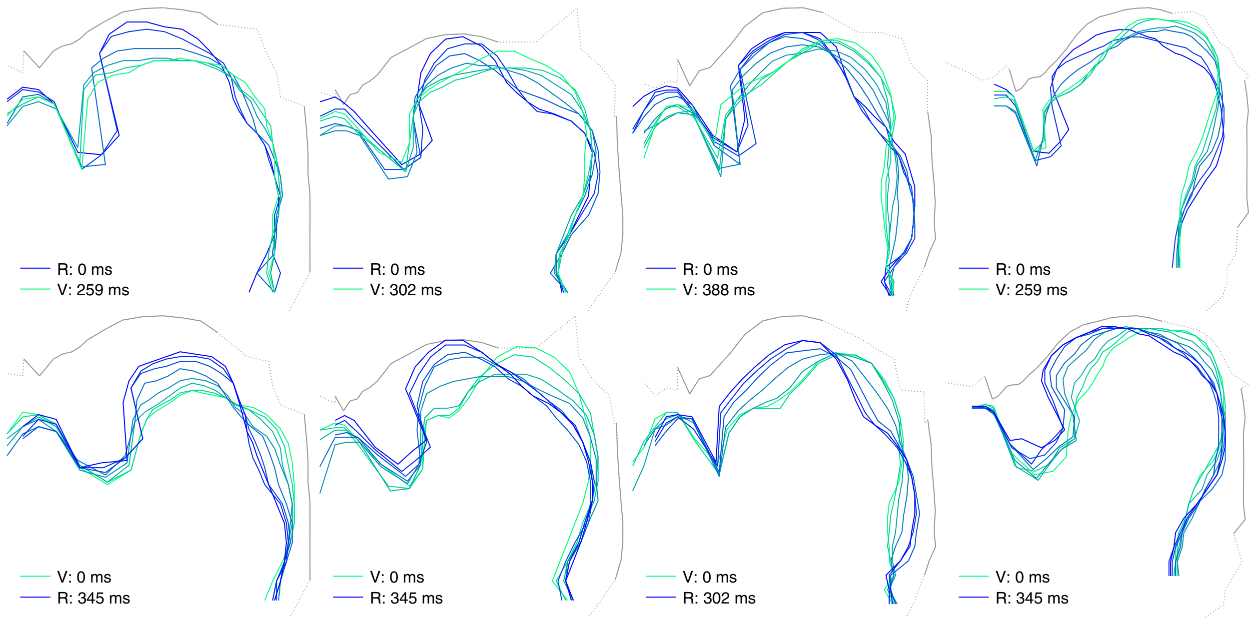


**Fig. 15.** Rhotic production in back vowel context. Top row: onset (*'robe'*); Bottom row: coda (*'bore'*); Left-to-right: W1, W2, W3, M1; Blue lines: tongue posture at rhotic coronal target; Green lines: vowel target posture. Intermediate colors: tongue postures captured at 43 ms intervals in the transition between rhotic and vowel. (For interpretation of the references to colour in this figure legend, the reader is referred to the web version of this article.)

fers from the pharyngeal posture at the vowel target. The saddle formed in the middle of the tongue between coronal and dorsal constrictions at the [ɹ] target is especially notable in rhotic production sequences in back vowel contexts because it coincides with the vowel constriction location. /oʊɹ/ rimes are articulated by lowering of the tongue from a vowel target constriction formed with a monolithic bunched gesture of the whole tongue, and creation of separate constrictions in the pharynx and the palate (Fig. 15, bottom row). Similar patterns of articulation to those illustrated in Figs. 14 and 15 are observed for liquids produced in /ʊ/ ('*loof*', '*pull*', '*boor*'), and /u/ ('*loop*', '*pool*', '*rube*') contexts.

### *3.5. Coarticulatory resistance of liquid consonants*

Articulatory target postures were compared for liquid consonants produced in different vowel contexts, using the method illustrated in Fig. 4. Mean lingual displacement across 30 laterals and 30 rhotics produced by each speaker are compared in Table 5. Each cell shows mean displacement within a set of 15 tongue outlines from the mean lingual posture calculated over that set. For each liquid at each syllable margin, mean displacement was calculated at the dorsal target of the consonant, in two different coarticulatory environments: adjacent to a set that we labeled 'tense' vowels [i-eɪ-ɑ-o-u], and a set that we labeled 'lax' vowels [ɪ-ɛ-ɑ-o-ʊ]. Each comparison was made within one of the (partially overlapping) sets of five vowels that can appear (and neutralize) before a coda rhotic, so that estimates of coarticulatory resistance were balanced in the number of tokens and the range of vowel qualities influencing articulation of the target liquid over the entire vowel space. To balance the sets, it was necessary to include the low back vowel and the mid back round vowel in both groups. As discussed in Section 2.2, in pre-lateral and pre-rhotic contexts, the mid back round vowel may be realized as [o(ʊ)] or [ɔ], depending on speaker and context. For Speaker W1, for example, the 15 onset laterals occurring before tense vowels (3 repetitions each of '*leap*', '*lame*', '*lob*', '*lobe*', '*loop*') were displaced from the mean midsagittal posture of the set by an average of 2.8 mm (per analysis gridline), over the length of the tongue from the sublingual cavity to the base of the epiglottis (Table 5, top left).

**Table 5**
Mean lingual displacement due to coarticulatory influence of adjacent vowels. Mean total displacement (s.d.) in mm/gridline from mean posture at dorsal target of liquid.

| | Vowel | Onset | | Coda | |
|---|---|---|---|---|---|
| | Set | Lateral | Rhotic | Lateral | Rhotic |
| W1 | [i-eɪ-ɑ-o-u] | 2.8 (1.1) | 1.5 (0.4) | 2.1 (0.9) | 1.4 (0.4) |
| | [ɪ-ɛ-ɑ-o-ʊ] | 2.6 (0.9) | 1.5 (0.4) | 1.9 (0.6) | |
| W2 | [i-eɪ-ɑ-o-u] | 1.4 (0.4) | 1.1 (0.3) | 2.4 (0.8) | 1.0 (0.2) |
| | [ɪ-ɛ-ɑ-o-ʊ] | 1.4 (0.5) | 1.1 (0.1) | 2.2 (0.6) | |
| W3 | [i-eɪ-ɑ-o-u] | 1.3 (0.5) | 1.6 (0.4) | 2.5 (0.9) | 1.8 (0.3) |
| | [ɪ-ɛ-ɑ-o-ʊ] | 1.1 (0.3) | 1.4 (0.5) | 2.3 (0.9) | |
| M1 | [i-eɪ-ɑ-o-u] | 1.9 (0.6) | 1.2 (0.3) | 1.5 (0.4) | 1.1 (0.4) |
| | [ɪ-ɛ-ɑ-o-ʊ] | 1.8 (0.6) | 1.3 (0.3) | 1.4 (0.4) | |
| Mean | | 1.8 (0.6) | 1.3 (0.2) | 2.0 (0.4) | 1.3 (0.3) |

Word-initial liquids vary in their resistance to coarticulatory influence by neighboring vowels. W3's onset laterals are more resistant to coarticulation before both tense and lax vowels than her onset rhotics (Table 5, row 3). For the other three participants, onset rhotics are produced with less displacement from mean lingual posture than onset laterals in each set of vowel contexts. For all four speakers, coda rhotics are less displaced from their common posture at the dorsal target than laterals produced after the equivalent vowels (Fig. 16).

A linear mixed model was constructed to examine the interaction of liquid type and position on lingual displacement due to vocalic coarticulation. Log lingual displacement (mm/gridline) was modelled as a function of consonant and syllable

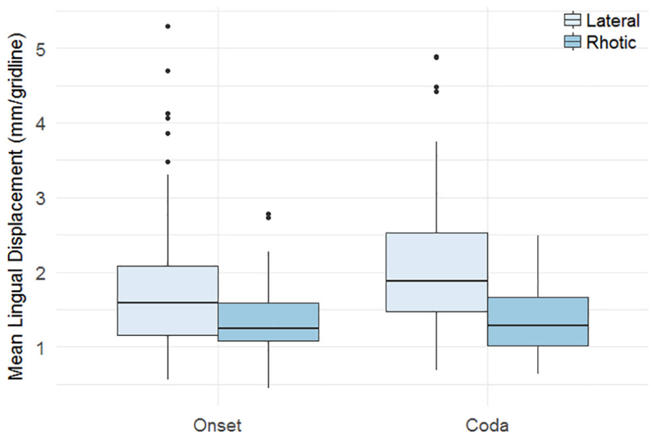


**Fig. 16.** Mean lingual displacement at liquid dorsal target. Mean displacement (mm/gridline), all speakers: 120 word-intial laterals vs. 120 word-intial rhotics; 120 word-final laterals vs. 120 word-final rhotics.

position with random effects for speaker. A model including by-speaker random slopes for consonant and position provided a better fit to the data compared to the model with random intercepts only ($\chi^2(1) = 103$, $p < 0.001$). Consonant type was treatment coded as Lateral = 0; Rhotic = 1. Syllable Position was coded as Coda = 0; Onset = 1 (details in Table C1). Rhotics were displaced less than laterals ($\beta = -0.41$, $t(3.4) = -3.3$, $p = 0.037$; $d = -0.85$, power = 46.2%), and there was an interaction between consonant and position, with liquids displaced less in onsets ($\beta = 0.19$, $t(467) = 3.39$, $p = 0.0008$; $d = 0.39$, power = 91.5%). Type III ANOVA of the model with Satterthwaite's method shows a main interaction between consonant and position ($F(1,467) = 11.5$, $p = 0.0008$) and a smaller effect of consonant ($F(1, 3) = 7.1$, $p = 0.076$). These results should be interpreted with caution, given the sparsity of data per speaker due to the aggregated metric used to quantify lingual displacement: the data are underpowered with respect to the overall effect of consonant, but well powered with respect to the interaction between consonant and position.

Bearing in mind these caveats, these data are consistent with the hypothesis that rhotics are produced with more consistent tongue shaping than laterals, while also revealing that individual speakers differ in the ways that vowels and liquids interact. Greater differences between liquids are observed in codas, and the data in Table 5 reflect different types of coarticulatory behavior in coda liquids. Articulatory variability can be seen across the whole length of the tongue in the word-final laterals produced by speakers W1 and W2 (Fig. 17, left-most panels). Coda laterals vary most across vowel contexts for W3, but the back of her tongue body remains relatively stable compared to the greater displacement of the tongue tip and blade between tokens (Fig. 17, 3rd panel). M1's word-final laterals show the least variability at the dorsal target, primarily varying in the height of the top part of the dorsum (Fig. 17, right-most panel). Coda laterals produced by all four speakers are characterized by a region of local maximal coarticulatory variability at the tongue tip, which increases with the overall degree of lateral vocalization.

Speakers W2 and M1 show the greatest consistency in production of word final rhotics (Fig. 18: panels 2 and 4). Coda rhotics of both speakers are highly stable at the back of the tongue, with very little variability across vowel contexts from the tongue root to the front part of the dorsum. Coda rhotics varied most across vowel contexts for W3, followed by W1 (Table 5, last column). The majority of this variability arises from differences in articulation of the saddle between the coronal and dorsal constrictions, and in the height and degree of fronting of the coronal gesture (Fig. 18, 1st and 3rd panels). Compared to the coda laterals, word-final rhotics are characterized by much less coronal coarticulatory variability. No speaker's coda rhotics vary more than 8 mm (max. Euclidean displacement) in tongue tip posture at the dorsal target (W3: '*bar*' vs. '*beer*'), whereas coda laterals differ as much as 18 mm in tongue tip articulation across tokens produced after different vowels (W1: '*pill*' vs. '*pull*').

### 3.6. Coarticulatory influence of liquid consonants

The influence of onset liquids on five different vowels is compared in Table 6. Each value – calculated using the method illustrated in Fig. 3 – indicates total lingual displacement (mm/gridline) from intrinsic vowel posture (captured in an inter-labial environment), in vowels produced after each consonant. Lingual displacement is calculated for each vowel which appears before coda rhotics (the most restricted environment: Table 2), allowing for direct comparison of both liquids in each syllable margin. Because these five vowel qualities are articulatorily dispersed throughout the vowel space, the mean values tabulated in the bottom row of each table therefore provide an estimate of the overall coarticulatory influence of each liquid on tautosyllabic vowels.

The influence of coda liquids on preceding vowels is compared using the same metric in Table 7. Each cell compares mean tongue posture at the target frame of a vowel in a

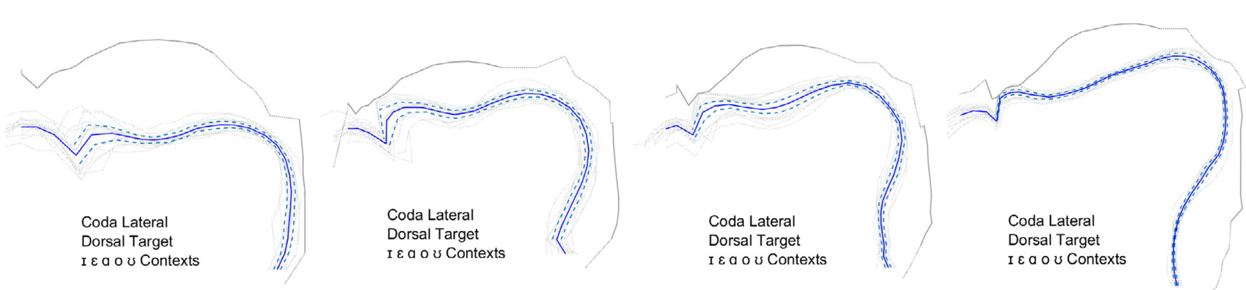


**Fig. 17.** Articulatory variability in coda laterals. Midsagittal tongue posture in 15 word-final laterals: 3 repetitions each of '*pill*', '*bell*', '*ball*', '*pole*', and '*pull*'. Left-to-right: Subjects W1, W2, W3, M1; Grey lines: lateral posture captured at dorsal target in each token; Blue solid lines: mean coda lateral tongue posture; Blue dashed lines: 2 s.d. from mean posture. (For interpretation of the references to colour in this figure legend, the reader is referred to the web version of this article.)

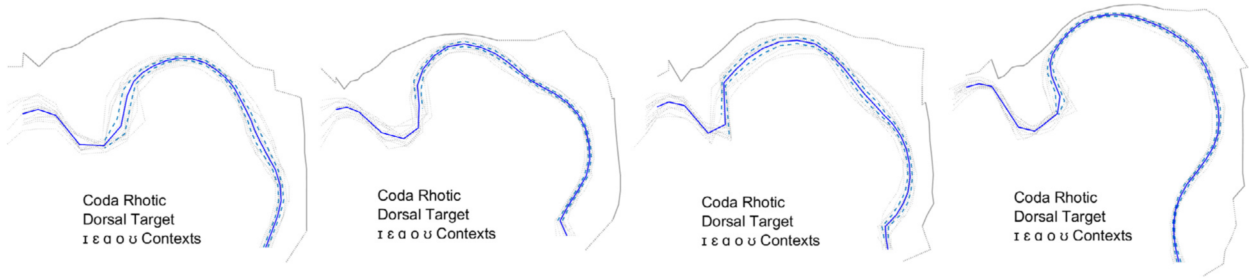


**Fig. 18.** Articulatory variability in coda rhotics. Midsagittal tongue posture in 15 word-final rhotics: 3 repetitions each of '*beer*', '*bare*', '*bar*', '*bore*', and '*boor*'. Left-to-right: Subjects W1, W2, W3, M1; Grey lines: rhotic posture captured at dorsal target in each token; Blue solid lines: mean coda rhotic tongue posture; Blue dashed lines: 2 s.d. from mean posture. (For interpretation of the references to colour in this figure legend, the reader is referred to the web version of this article.)

**Table 6**
Vocalic deformation (mm/gridline) due to coarticulatory influence of onset liquids.

| | Lateral | | | | | Rhotic | | | |
|---|---|---|---|---|---|---|---|---|---|
| | W1 | W2 | W3 | M1 | | W1 | W2 | W3 | M1 |
| [lɪ-] | 0.7 | 0.8 | 0.6 | 0.6 | [ɹɪ-] | 0.6 | 0.8 | 0.8 | 0.5 |
| [lɛ-] | 1.1 | 0.5 | 0.4 | 0.4 | [ɹɛ-] | 0.6 | 0.6 | 0.3 | 0.3 |
| [lɑ-] | 0.4 | 0.8 | 0.2 | 0.6 | [ɹɑ-] | 0.7 | 0.6 | 0.2 | 0.3 |
| [loʊ̆-] | 0.6 | 0.6 | 0.9 | 0.5 | [ɹoʊ̆-] | 0.8 | 0.6 | 0.8 | 0.5 |
| [lʊ̆-] | 0.6 | 0.6 | 0.5 | 0.5 | [ɹʊ̆-] | 1.5 | 1.1 | 1.3 | 1.0 |
| Mean | 0.7 | 0.7 | 0.7 | 0.5 | Mean | 0.8 | 0.7 | 0.7 | 0.5 |

**Table 7**
Vocalic deformation (mm/gridline) due to coarticulatory influence of coda liquids.

| | Lateral | | | | | Rhotic | | | |
|---|---|---|---|---|---|---|---|---|---|
| | W1 | W2 | W3 | M1 | | W1 | W2 | W3 | M1 |
| [-ɪl] | 0.4 | 0.6 | 0.4 | 0.7 | [-ɪɹ] | 1.1 | 0.8 | 0.4 | 0.6 |
| [-ɛl] | 0.4 | 0.6 | 0.2 | 0.6 | [-ɛɹ] | 1.3 | 0.6 | 0.9 | 1.0 |
| [-ɑl] | 0.4 | 0.8 | 0.3 | 0.6 | [-ɑɹ] | 0.6 | 0.8 | 0.4 | 0.8 |
| [-ol] | 0.7 | 0.8 | 0.4 | 1.1 | [-oɹ] | 1.0 | 1.0 | 0.2 | 1.1 |
| [-ʊ̆l] | 0.7 | 0.6 | 0.6 | 0.8 | [-ʊ̆ɹ] | 1.5 | 1.8 | 0.5 | 1.5 |
| Mean | 0.5 | 0.7 | 0.4 | 0.7 | Mean | 1.1 | 0.9 | 0.5 | 1.0 |

liquid-final rime with the mean posture of the reference vowel repeated between two labial consonants, and indicates the total displacement (mm/gridline) between the two midsagittal lingual outlines. For speaker W1, for example, the mean vowel shape at the nucleus of '*pill*' is displaced 0.4 mm/gridline from the target tongue posture in '*bib*' (Table 7, top left), while the tongue is displaced 1.1 mm/gridline from the reference interlabial vowel posture in the equivalent vowel before a coda rhotic in the word '*beer*'. Our choice of comparison vowel in interlabial context is the set [ɪ-ɛ-ɑ-o-ʊ], because the coarticulatory aggression data show that pre-coda vowels were less displaced from the un-coarticulated lax vowel set compared to the tense vowel comparisons (Table 5). The quality of vowels appearing before coda rhotics is not always clear, since tense/lax contrasts are neutralized in this environment. Nevertheless, we have good reason to believe that in the dialect of the study participants, as for most speakers of General American English, a non-diphthongal variant occurs in this environment (not [eɪ], [oʊ], [i$^j$], or [u$^w$]), and that the reference vowels are sufficiently close to those before /ɹ/ to make a valid basis of comparison.

A linear mixed model was constructed to examine the interaction of liquid type and position on lingual displacement in vowels. Vocalic deformation (mm/gridline) was modelled as a function of consonant and syllable position with random effects for speaker. A model including by-speaker random slopes for position provided a better fit to the data compared to the model with random intercepts only ($\chi^2(1) = 6.7$, $p = 0.03$). Consonant type was treatment coded as Lateral = 0; Rhotic = 1. Syllable Position was coded as Coda = 0; Onset = 1 (details in Table C2). Rhotics had a greater effect on vowel displacement than laterals ($\beta = 0.29$, $t(70) = 3.73$, $p = 0.001$; $d = 0.90$, power = 89.8%), and the effect of consonant was greater in coda position ($\beta = 0.22$, $t(70) = 1.98$, $p = 0.051$; $d = 0.68$, power = 50.6%). Type III ANOVA of the model with Satterthwaite's method shows a main effect of consonant ($F(1, 70) = 10.8$, $p = 0.002$) and a smaller interaction between consonant and position ($F(1,70) = 3.95$, $p = 0.051$). These results should be interpreted with caution, given the sparsity of data per speaker due to the aggregated metric used to quantify vocalic deformation: the data are underpowered with respect to the interaction between consonant and position, but well powered with respect to the overall effect of consonant on vowel articulation.

Bearing in mind these caveats, these data suggest that overall for these four speakers, coda rhotics have a greater influence on a vowel in the same syllable than both onset rhotics and onset laterals; however, the relative influence of liquids on a specific vowel also varies across speakers. In particular, there is greater deformation of pre-lateral vowels compared to pre-rhotic equivalents for W3 '*pole*' > '*bore*', W3 '*pull*' > '*boor*', and M1 '*pill*' > '*beer*'. For all other rimes, a coda rhotic has the same or more influence on the preceding vowel than a lateral (Fig. 19).

### *3.7. Summary of main findings*

Midsagittal articulation of rhotic and lateral approximants by four speakers was compared in all phonotactic environments where liquid consonants occur in General American English syllables with simple margins. The main findings of this study, with respect to intergestural coordination, are:

i. in **onset laterals**, the coronal gesture was achieved before the dorsal gesture reached its target in all vowel contexts; maximum TB retraction was achieved, on average, 190 ms after TT closure/maximum advancement
ii. lingual gestures were sequenced in the reverse order in **coda laterals**, but complete midsagittal tongue tip closure was only observed in 54% of 120 lateral-final words; maximum TB retraction was achieved approximately 150 ms before TT closure/maximum advancement
iii. **onset rhotics** were produced with synchronous coronal and dorsal gestures, preceded by labial approximation/protrusion (mean 20 ms before the lingual gestures)
iv. in **coda rhotics**, the posterior lingual gesture preceded the coronal gesture by 80 ms (mean across all vowel contexts); no evidence of a labial gesture was found in word-final rhotics

The main findings of this study, with respect to patterns of liquid co-production, are:

i. rhotics showed greater **consistency in target posture** across syllable positions than laterals, which displayed greater articulatory differences between onset and coda variants
ii. rhotics showed greater **resistance to coarticulation** across vowel contexts than laterals: lingual displacement from mean posture was significantly lower for rhotics compared to laterals at both syllable margins

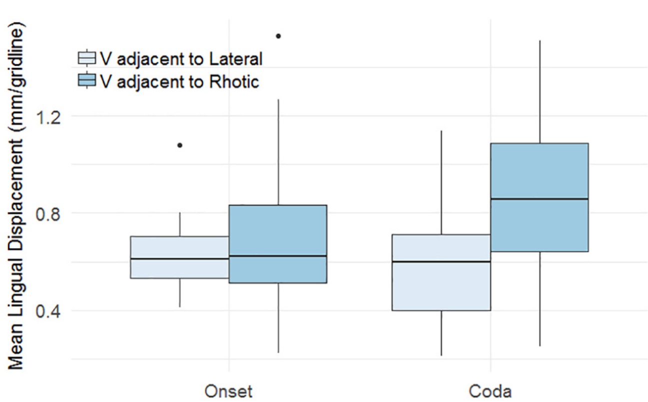


**Fig. 19.** Mean lingual displacement at vowel target from default vowel posture: lax vowels adjacent to liquids. Mean lingual posture of vowels produced after/before liquid consonants (three repetitions of each of five vowels), compared to mean posture of same vowels produced in inter-labial contexts (two repetitions). Euclidean distances between two tongue shapes calculated from tongue root to sub-lingual cavity, averaged across all speakers (mm/grid line).

iii. vowels adjacent to rhotics were significantly more displaced from construed target postures than when produced adjacent to laterals. Coda rhotics induced greater displacement, consistent with exertion of the greatest **coarticulatory influence** on tautosyllabic vowels

## 4. Discussion

The articulatory characterization of liquids based on these data is broadly consistent with previous studies. However, some new insights emerge from the more complete picture of the vocal tract afforded by rtMRI, and from comparing the ways that liquids coarticulate in previously unexamined environments. The rtMRI data reveal the importance of studying liquid consonant production in a wide range of positional and vowel contexts, to more fully understand the interaction of the intrinsic gestures of the liquids with those of the surrounding sounds, and how these may differ across individuals (see Mielke, Baker, & Archangeli, 2016).

### *4.1. Characterizing multigestural segments*

An important methodological insight reinforced by these data is that there is no single timepoint at which all phonetic features of laterals or rhotics can be robustly characterized or consistently compared across all contexts and speakers. Previous studies have reported key phonetic parameters of liquids captured at a single point in time, assumed to be the consonantal target. All formant values in Bladon and Al Bamerni (1976), for example, were measured at "each occurrence of /l/" (p. 139), and Giles and Moll (1975) compare allophonic variants of laterals from composite images acquired "during steady-state configurations . . .in which the positions of both the tongue apex and dorsum were invariant" (p. 210). These rtMRI data reveal that speakers rarely achieve articulatory steady states during liquid production, and that target consonantal postures may not be directly comparable across speakers because of individual differences in realization and coordination. Even for onset rhotics – the liquid allophone in which lingual gestures are most consistently synchronized – a single target frame cannot be consistently identified because maximum labial approximation typically leads lingual accomplishment. Attempts to compare liquid parameters at a single goal – such as maximum lingual elongation – were therefore abandoned in this study in favor of separate analyses at coronal and dorsal landmarks.

### *4.2. Lateral goals of production*

Mean lateral tongue shapes for speakers M1, W3 and W2 (Fig. 6) closely resemble those of subjects A, B and C respectively, in the study by Giles and Moll (1975). All W1's laterals, on the other hand, show the dorsum to be considerably lower than the tongue tip at the landmark of the coronal target, unlike the other three speakers in this study and all speakers imaged by Giles and Moll (1975). Speaker JO in the ultrasound study of Lee-Kim, Davidson, & Hwang, 2013 produces the laterals in '*tallest*' and '*flawless*' with a dorsum marginally lower than the tongue tip, but all other laterals in that six-speaker study appear to be articulated with the back of the tongue at least as high as the tongue tip.

Leidner (1976) observed in an electromyograph study of two speakers of American English that less muscle activity was involved in lateral production after back vowels compared to front vowels, and characterized the lateral dorsal target as [u]-like. The patterns of coda lateral production examined here are consistent with Leidner (1976)'s findings in that they generally demonstrate less tongue body retraction in back vowel contexts. Dorsal targets in laterals produced by W2 and W3's closely resemble their [u] and [ʊ] vowels respectively, consistent with Leidner's (1976) and other characterizations (e.g. Hardcastle & Barry, 1989's) study of lateral vocalization in Southern British English. However, these MRI data show that the exact target of the lateral posterior gesture is speaker-specific and cannot always be characterized as velar. In particular, the lateral tongue body constriction location for W1 is very much lower than her dorsal target for [u], and more closely matches her [ɑ] (Fig. 12). M1's laterals also have a dorsal target that is lower and more retracted than the other speakers, and appears to be closer to his [ʌ].

### 4.3. Rhotic goals of production

The rhotics produced by all four speakers in this study have lingual postures which fit into established typologies of American English /ɹ/. In Delattre and Freeman's (1968) classification, W3's rhotic closely resembles Type 4, those produced by W1 and W2 match Types 5/6, and M1's rhotic resembles Types 1 to 3, in terms of global shaping. The positional allophony observed in these MRI data is consistent with the findings of Hagiwara (1994) that speakers with 'blade up' initial rhotics typically realize syllabic and final /ɹ/ with 'tip down' – i.e. less retroflexed or more bunched – tongue postures. The more bunched and rounded postures of the coda rhotics in our study also closely resemble the cineradiographic tracings of postvocalic [ɹ] presented in Lindau (1985).

Considerable interspeaker variability was observed in the location of the pharyngeal constriction for /ɹ/ in these data (Section 3.2). Similar variability can also be seen among Lindau's (1985) six speakers of American English: the lowest constriction in that study was formed with the epiglottis in the lowest part of the pharynx (P5), at a similar location to W1's coda rhotic (Fig. 7), and Lindau's (1985) speakers P2, P3, and P6 all articulate the rhotic in '*herd*' with a mid-pharyngeal TB constriction similar to that of W2. The primary posterior constriction of M1's rhotic was strikingly high across both syllable positions and all vowel contexts: approximately 30 mm higher than the mid-pharyngeal constriction of W2, and closer to the uvular than the glottis. M1's rhotic appears to have a pharyngeal constriction target located further from the glottis than that of most other American English speakers for which rich imaging data of the pharynx is available (Alwan, Narayanan, & Haker, 1997; Delattre & Freeman, 1968; Espy-Wilson, Boyce, Jackson, Narayanan, & Alwan, 2000; Lindau, 1985; Zhou et al., 2008).

Although some activity in the epiglottal region was observed during rhotic production by all speakers, neither M1 nor W2 has a rhotic in which the narrowest part of the pharyngeal constriction is formed with the tongue root (cf. Gick & Campbell, 2003). These data suggest that the posterior rhotic gesture is better characterized as dorsal: regardless of the specific constriction location, it is formed between the back of the tongue body and the rear pharyngeal wall (Alwan, Narayanan, & Haker, 1997; Espy-Wilson, Boyce, Jackson, Narayanan, & Alwan, 2000). It should be noted again that all midsagittal lingual profiles in this study were traced along the back of the tongue inside the epiglottis for consistency across frames and speakers, so exact comparisons of articulation in the lower pharyngeal region with X-ray, cineradiographic, and ultrasound studies that trace the lower dorsum outside the epiglottis are not always possible.

### 4.4. Patterns of coarticulation

This study has revealed differences in the coarticulatory properties of liquids that may influence their phonological behavior. Rhotics were more resistant to coarticulatory influence than laterals at both syllable margins, but the contrast between coda consonants was greater in this respect (Fig. 16). In addition, rhotics were found to exert more coarticulatory influence on adjacent vowels, especially in codas (Fig. 19). These coarticulatory patterns are consistent with the predictions of our hypothesis that rhotics are represented with a dorsal gesture with a higher specified blending strength than that of laterals in General American English; however, these findings should be interpreted with caution, given the limited number of participants in this study.

Since there is no tense-lax vowel contrast before coda rhotics, one possible account of these findings is that the differences in tongue shaping before rhotics arise because the vowel in this context is actually a different quality with a different articulatory target to the comparison vowel elicited in the labial coda context. This is a more extreme case of the general problem of categorizing and comparing vowel quality across different words and contexts: some vowel quality differences are also reduced in pre-lateral environments, for example, and there may be sound changes involving mergers of some pre-lateral vowel contrasts in progress for some speakers (Labov et al., 2005). Nevertheless, the metrics explored here offer useful insights into the relative coarticulatory influences of liquids in different positions because they make reference to the entire vowel space, rather than individual vowel qualities. Further evidence for the idea that rhotics are characterized by greater coarticulatory dominance than laterals comes from their behavior in onsets, where they were found to be more resistant to coarticulatory deformation than laterals (Section 3.5). Furthermore, although the differences in coarticulatory aggression between liquids were greatest in codas (based on the construed vowel targets), rhotics were also significantly more influential on adjacent vowel posture overall – i.e. across both syllable margins (Section 3.6). Collectively, this suggests that these data are not merely artifacts resulting from measuring vowels already neutralized to a different quality before coda rhotics.

If these patterns hold for other speakers of American English, they may be factors in the restriction of vowel qualities before coda rhotics. Tense-lax contrasts, for example, may be harder to maintain in a pre-rhotic environment where the consonant exercises greater influence on the nuclear vowel. Coda laterals, if more adaptable and less coarticulatorily aggressive, would be more likely to support a greater variety of vowel qualities in their rimes, including fine contrasts. These data also shed more light on the question of vowel identity before coda rhotics (Giegerich, 1992; Hammond, 1999). The patterns of coarticulation observed here are consistent with the analysis of Kenyon and Knott (1953) and Wells (1982), 481–485, who argue that lax variants appear before rhotics in General American English. Vowels produced in this environment might be more centralized if a following rhotic exerts greater influence on the tongue body, resisting vowel movement to more peripheral targets or to targets more displaced from the intrinsic dorsal posture associated with an individual speaker's rhotic.

This raises further questions about the broader mechanisms by which such intergestural relationships might condition vowel neutralization among individuals in a speech community. We are not committed to whether such neutralization phenomena are synchronic or diachronic, or both. Nevertheless, the patterns identified in Section 1 are systematic across the General American English lexicon. While a phonological analysis goes beyond the scope of this paper, we suggest that our phonetic investigation can provide insight into the gestural representation that gives rise to this pattern that could inform a phonological account. Walker & Proctor, 2013 have described some phonological properties of rhotic-initial complex codas in General American English which may be influenced by articulatory properties of vowel-rhotic-consonant sequences.

### 4.5. Patterns of gestural coordination

The basic patterns of gestural coordination observed in these rtMRI data are largely consistent with those described in previous studies, however the magnitude and details of some intergestural timings differ. Gick & Campbell, 2003 also reported a positive lag of similar magnitude (10–20 ms) between the labial and lingual gestures of initial rhotics produced by eight speakers of American and other varieties of English, but found the lingual (and labial) gestures of coda rhotics to be near-synchronous. A longer and more consistent lag between lingual gestures was observed in word-final rhotics in this study: the tongue body/root gesture preceded the anterior constriction by 80 ms on average. Gick et al. (2006) found no lag between the lingual gestures of Western Canadian laterals in both pre- and post-vocalic positions. Three key differences between these studies may account for these discrepancies. Final rhotics in this study were compared across a greater range of vowel contexts ([ɪ-ɛ-ɑ-o-ʊ] vs. [i-a]), our experimental corpus was elicited with single word utterances (rather than in a carrier phrase), and the locations at which lingual constrictions were measured differed. MRI more consistently reveals more of the lower pharynx than ultrasound, which allowed us to measure the posterior gesture of the rhotic closer to the tongue root, where articulation may vary from other regions at the back of the dorsum.

Inter-gestural timings in these data are also longer than those reported for Scottish and Southern British English laterals (Scobbie & Pouplier, 2010). Mean lag between achievement of alveolar constriction and beginning of dorsal retraction in that study did not exceed 66 ms word-initially, and 126 ms for word-final laterals. Methodological differences would also appear to be the most likely cause of this discrepancy. Different gestural landmarks were used in Scobbie & Pouplier, 2010 study, and timing data were determined from patterns of EPG contact which indirectly gauge tongue body retraction, and may not be directly comparable with rtMRI measurements tracking tissue boundaries. Most importantly, those laterals were elicited in full sentences, which will shorten timings compared to the longer durations of the isolated word utterances we used in this study.

Furthermore, when we consider only the intergestural timings of laterals elicited in the most comparable vowel context to that used in Scobbie & Pouplier, 2010 – '*leap*'-'*peel*' – we find similar lags for some speakers, and variability that reflects individual speaker differences in lateral articulation. W1 has a much longer mean coda lateral lag (TT–TB = 273 ms) in high front vowel contexts than the other three speakers (mean 67 ms), which may result in part from her more retracted lateral dorsal target. For this speaker, lateralization of the tongue in the rime of '*peel*' requires greater dorsal excursion from the palatal target of the nucleus towards an [ɑ]-like target, compared to higher, fronter lateral dorsal targets of the other speakers in this study.

### 4.6. Patterns of vowel-liquid interaction

A motivating goal of this study was to shed more light on asymmetries in the ways that liquids restrict and interact with vowels in English rimes. To facilitate examination of these issues, mean lags between lingual gestures for both liquids have been recalculated from Tables 3 and 4 and plotted together in Fig. 20 for comparison. Laterals at both syllable margins show greater mean temporal displacement between achievement of coronal and dorsal goals compared to rhotics produced in the same positions. This greater intergestural lag means that more time is available for articulators to move between tasks. The phonetic basis for this lag difference remains an open question. One possibility is that laterals and rhotics might differ in the relative independence of their coronal and dorsal gestures in temporal and/or spatial dimensions.

For the speakers in this study, it is not only the lag between coronal and dorsal gestures that differs systematically between liquids, but also the relative lag between the dorsal gestures of the vowel and liquid. At both syllable margins, TB–V duration is

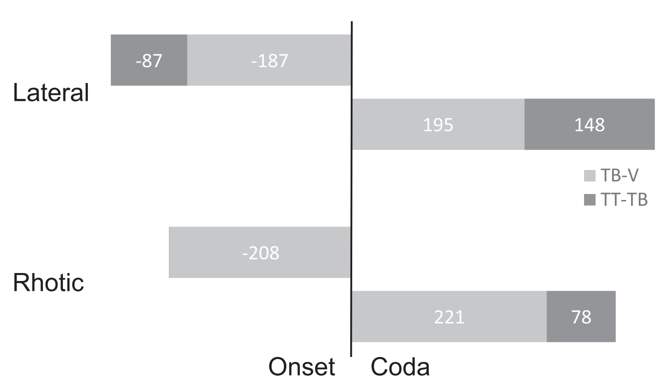


**Fig. 20.** Mean lags between lingual gestures. Mean lags (ms, all speakers) between achievement of coronal and dorsal gestures (TT–TB), and dorsal and vowel gestures (TB–V). Negative lags (left): intergestural timing for onset liquids; Positive lags (right): intergestural timing for coda liquids. TT-TB lag is zero for onset rhotics.

longer for rhotics than laterals, and it constitutes a greater proportion of the total articulatory duration (TT–V) compared to the longer laterals. It is possible that the longer mean transition between the vowel target and the dorsal target of the following rhotic is related to the greater exertion of coarticulatory dominance by rhotics if the production of rhotics is controlled to reduce the potential for articulatory interaction with adjacent vowels. In a gestural representation, this could possibly be understood in terms of minimizing temporal overlap between a vowel and the dorsal gesture of a coda liquid with a high blending strength specification.

Vowel quality could be expected to interact with TB–V duration in such a way that a longer mean transition is expected in rimes with vowels for which the tongue body gesture is more incompatible with that of the liquid. This is borne out in our data in rimes with laterals. A linear mixed model was constructed to examine the effect of vowel quality on TB–V lag in lateral codas. TB–V lag was modelled as a function of vowel backness with random intercepts for speaker (details in Table B6). Front vowels [i-ɪ-eɪ-ɛ-æ] had a greater effect on TB–V lag than back vowels [ʌ-ɑ-oʊ-ʊ-u], increasing it by 94 ms ($\beta = 94.4$, $t(115) = 8.79$, $p < 0.001$; $d = 1.24$, POWER = 100%). The influence of vowel quality on TB–V lag in coda rhotics cannot be reliably modelled in the same way in these data due to sparsity and imbalance in the equivalent subset of rhotic-final rimes, but this would be valuable to examine in a future study. An important consideration for this type of analysis is what constitutes a 'compatible' tongue body gesture: the data illustrated in Figs. 9, 11, 13 and 15 reveal that even for back vowels, different vowel qualities map more closely onto the rhotic postures produced by different speakers at the dorsal target; for laterals, on the other hand, it is largely backness that appears to distinguish vowels that are matched with the dorsal posture of liquid (Figs. 8, 10, 12 and 14).

Collectively, these data suggest that laterals may have a greater adaptability in the ways that they can combine with vowels compared to rhotics. Overall, according to these methods of comparison of tongue shape and intergestural timing, the laterals produced by these speakers exert less dominance on the vowels they coarticulate with, and it is possible that lingual gestures in a lateral may be more independent. Both of these properties may allow the lateral greater freedom to combine phonotactically with a wider range of segments than rhotics, including those with gestures specified for goals which differ from those of the liquid.

### 4.7. Implications for models of syllable structure

These data raise some important questions about gestural organization in syllables, and coordination in syllable rimes in particular. Brunner, Geng, Sotiropoulou, and Gafos (2014) and Pouplier (2012) have proposed that timing relationships between a consonant and tautosyllabic vowel depend on the coarticulatory properties of the consonant. Evidence for this was provided by an EMA analysis of Polish onset cluster production (Pastätter & Pouplier, 2017), which revealed that sibilants and alveolar sonorants show less overlap with a following vowel compared to labials, consistent with the hypothesis that the degree of overlap in a CV sequence is a function of the intrinsic coarticulatory resistance of the consonant. This proposal is consistent with our finding that the consonant exhibiting the greater stability against coarticulatory influence from vowels – the rhotic – shows a greater mean lag between the achievement of its tongue body gesture and that of the preceding vowel (Fig. 20). A greater lag could be interpreted as an indirect measure of less gestural overlap, because it indicates a greater duration between achievement of gestural targets, suggesting there is less dorsal overlap in a rhotic-final rime. On the other hand, if the TT–TB lag is also considered, the lags in Fig. 20 suggest that the liquid characterized by lower coarticulatory resistance according to the rtMRI analysis – the lateral – shows less *overall* overlap with the preceding vowel in a rime.

There are important differences between this study and that of Pastätter and Pouplier (2017). Most critically, their study examined complex onsets – which are hypothesized to be in a synchronous relationship with the tautosyllabic vowel – while we focused on simplex codas, which are assumed to be coupled asynchronously to the preceding vowel (Browman & Goldstein, 1992). Coarticulatory influences on temporal displacement around the C-center in a syllable onset (Browman & Goldstein, 1988) might differ in important ways from temporal reorganization in an anti-phase coda. Furthermore, the English liquids compared in this study both consist of tongue body gestures, while Pastätter and Pouplier (2017) examined Polish labials, coronals, nasals, and a clear lateral, none of which may have a strong dorsal component (although see Proctor, 2011, on tongue body control in clear Spanish laterals). Although the relative coarticulatory properties of consonants have been examined in detail in Catalan and some other languages (etc. Recasens, 1984; Recasens & Espinosa, 2009; Recasens & Rodríguez, 2017), more work is required to understand how consonants specified for a tongue body gesture interact with adjacent segments in English.

The principles governing temporal organization in codas are still an active area of research. Data showing sequential organization of post-vocalic gestures in some languages is consistent with models in which coda segments are coupled anti-phase to the nucleus (Browman & Goldstein, 1995b; Krakow, 1999), but studies of coda clusters and multi-gestural segments reveal some more complex patterns of coordination in codas, which have given rise to alternative models (etc. Marin, 2013; Marin & Pouplier, 2010; Tilsen, 2016). The intergestural timing patterns revealed by these rtMRI data are broadly consistent with models of other multi-gestural segments in which a lingual gesture is coupled anti-phase with the nucleus, and a secondary gesture is coupled to that linking gesture – a model which has been used to account for timing patterns in English nasal codas (Byrd, Tobin, Bresch, & Narayanan, 2009). Yet liquids present a more complicated case in some respects than nasals, as the two primary constituent gestures are both lingual, raising the question of which gesture in a coda liquid would be coupled to a preceding vowel. Because intergestural timing in American English coda liquids broadly patterns with coda nasals, they could possibly be modelled as having the coronal gesture coupled anti-phase to the vowel (Byrd et al., 2009) – a model considered in more detail in Walker & Proctor, 2019. Marin and Pouplier (2010) compare evidence for different models of organization of coda laterals, including direct coupling of both lingual gestures to the preceding vowel. It remains an open question whether the different TB–TT lags observed between the liquids in this study arise from different additional coupling relationships or whether they are due to other intrinsic properties of each type of liquid, such as differences in constriction location or the formation of a side branch in the lateral. A related issue is whether principles of recoverability play into gestural organization (Byrd, 1996; Chitoran, Goldstein, & Byrd, 2002). More data obtained with greater temporal resolution from a greater number of speakers will be required to shed more light on these possibilities and to further investigate the influence of vowel quality on timing patterns.

### *4.8. Further considerations*

The data presented in this study are limited in some important respects. There are many more factors that have been shown to influence liquid production which could not be controlled or modelled in these data. In particular, lexical and morphological factors can influence liquid behaviour at a sub-segmental level, which may affect the way that these consonants interact with other elements in the rime. For example, Lin, Davies, Turpin, Ross, and Demuth (2014) found that word frequency has a greater effect on coronal articulation of American English laterals (more lenition in high-frequency words) than on the dorsal gesture, which remains relatively stable. Lee-Kim, Davidson, & Hwang, 2013 showed that stem-final word medial laterals (e.g. '*tall-est*') are not as dark as word- and stem-final allophones ('*tall*') in American English. Ultrasound data revealed that the most consistent articulatory correlate of lateral darkness for the speakers in that study of was tongue body lowering, which suggests that coda laterals might coarticulate differently with preceding vowels depending on the morphological context, as well as intrinsic coarticulatory blending factors.

### *4.9. Future directions*

More detailed phonetic characterization of coda liquids and the ways that they interact with different vowels will require information about articulation beyond the mid-sagittal plane. The use of parasagittal sensors in EMA analysis is providing new insights into the way that the sides of the tongue are coordinated with coronal and dorsal activity in the midsagittal plane (Ying et al., 2017), and new 3d rtMRI methods will offer further advantages in parasagittal sensing (e.g.Zhu, Kim, Proctor, Narayanan, & Nayak, 2013).

The default video reconstruction frame rate of these rtMRI data is not rapid enough to resolve some fine timing details of gestural coordination, especially near-synchronous articulatory activity. Although temporal resolution could be improved in the existing data using alternative video reconstruction techniques (e.g. Proctor, Lo, & Narayanan, 2015), future studies of intergestural timing and coarticulation in liquids will be better served by new rtMRI sequences offering greater temporal and spatial resolution (e.g. Lingala et al., 2017).

This study has identified some patterns of coarticulation and intergestural timing which might arise from hypothesized differences in blending strength in the gestural representation of liquids. A more complete understanding of the specified blending strength of English liquid consonants and the dynamics of their interactions with vowels will require more data about tongue shaping and gestural timing in vowel-liquid rimes produced by more speakers, as well as modelling. TADA – an implementation of the Task Dynamic model of inter-articulator coordination in speech (Nam, Goldstein, Saltzman, & Byrd, 2004) – allows manipulation of constriction location and degree, and blending strength specifications for the gestures in an utterance, and simulation of the resulting articulatory dynamics (Nam et al., 2006). It is beyond the scope of the current study to model the effects of blending strength and vowel quality on liquid interactions with adjacent vowels, but these parameters should be systematically manipulated in a series of TADA simulations to test these ideas further.

## Declaration of Competing Interest

The authors declare that there is no conflict of interest regarding the publication of this article.


## Acknowledgements

This work was supported by National Institutes of Health grant NIH Grant R01 DC007124; and Australian Research Council Award DE150100318. We are grateful to Taehong Cho and three anonymous reviewers for their comments on earlier drafts of this manuscript.


## Appendix A. Summary of statistical modeling: rhotic labial articulation

Statistics of linear mixed-effects models examining the effect of consonant type on labial articulation (Section 3.2) are summarised in Tables A1 and A2. Position coding: Coda = 0, Onset = 1. *p*-values are calculated with the *lmerTest*

**Table A1**
Rhotic labial aperture (mm) as a function of syllable position.

| MODEL: | $LA \sim Pos + (1\|Subj)$ | | | | |
|---|---|---|---|---|---|
| | RANDOM EFFECTS: | | | | |
| Groups | Name | | Variance | | S.D. |
| Subj | (Intercept) | | 12.53 | | 3.54 |
| Residual | | | 9.20 | | 3.03 |
| | Number of observations: 168, groups: Subj, 4 | | | | |
| | FIXED EFFECTS: | | | | |
| | Estimate | SE | df | t-value | Pr(>\|t\|) |
| (Intercept) | 14.90 | 1.81 | 3.2 | 8.22 | 0.003 |
| Pos-Ons | −9.17 | 0.49 | 163.0 | −18.77 | <2e − 16 |

**Table A2**
Rhotic labial protrusion (mm) as a function of syllable position.

| MODEL: | $LP \sim Pos + (1\|Subj)$ | | | | |
|---|---|---|---|---|---|
| | RANDOM EFFECTS: | | | | |
| Groups | Name | | Variance | | S.D. |
| Subj | (Intercept) | | 13.3 | | 3.7 |
| Residual | | | 9.0 | | 3.0 |
| | Number of observations: 168, groups: Subj, 4 | | | | |
| | FIXED EFFECTS: | | | | |
| | Estimate | SE | df | t-value | Pr(>\|t\|) |
| (Intercept) | 1.55 | 1.87 | 3.2 | 0.83 | 0.464 |
| Pos-Ons | 5.65 | 0.49 | 163.0 | 11.72 | <2e−16 |

**Table B1**
TT–V lag (ms) in Onsets.

Random Effects:

| Groups | Name | Variance | S.D. |
|---|---|---|---|
| Subj | (Intercept) | 124.6 | 11.3 |
| Residual | | 2495.7 | 50.0 |

Number of observations: 228, groups: Subj, 4

Fixed Effects:

| | Estimate | SE | df | t value | Pr(>\|t\|) |
|---|---|---|---|---|---|
| (Intercept) | −274.1 | 7.2 | 4.6 | −38.0 | 6.9e−07 |
| Cons-Rhotic | 66.1 | 6.6 | 223.0 | 10.0 | <2e−16 |

**Table B2**
TB–V lag (ms) in Onsets.

Random Effects:

| Groups | Name | Variance | S.D. |
|---|---|---|---|
| Subj | (Intercept) | 59.6 | 7.7 |
| Residual | | 2375.9 | 48.7 |

Number of observations: 228, groups: Subj, 4

Fixed Effects:

| | Estimate | SE | df | t value | Pr(>\|t\|) |
|---|---|---|---|---|---|
| (Intercept) | −187.5 | 5.9 | 5.6 | −31.8 | 1.44e−07 |
| Cons-Rhotic | −20.5 | 6.5 | 223.0 | −3.2 | 0.0018 |

package (Kuznetsova et al., 2017) using Satterthwaite's method of approximation.

## Appendix B. Summary of statistical modeling: intergestural timing

Statistics of linear mixed-effects models examining the effect of consonant type on intergestural timing relationships (Section 3.3) are summarised in Tables B1,B2,B3,B4,B5. Consonant coding used in all models: Lateral = 0 (Intercept), Rhotic = 1. *p*-values are calculated with the *lmerTest* package (Kuznetsova et al., 2017) using Satterthwaite's method of approximation.

**Table B3**
TT–V lag (ms) in Codas.

Random Effects:

| Groups | Name | Variance | S.D. |
|---|---|---|---|
| Subj | (Intercept) | 7040 | 83.9 |
| Residual | | 4167 | 64.6 |

Number of observations: 180, groups: Subj, 4

Fixed Effects:

| | Estimate | SE | df | t value | Pr(>\|t\|) |
|---|---|---|---|---|---|
| (Intercept) | 343.4 | 42.4 | 3.0 | 8.1 | 0.0037 |
| Cons-Rhotic | −44.3 | 10.2 | 175.0 | −4.3 | 2.45e−05 |

**Table B4**
TB–V lag (ms) in Codas.

Random Effects:

| Groups | Name | Variance | S.D. |
|---|---|---|---|
| Subj | (Intercept) | 1766 | 42.0 |
| Residual | | 4608 | 67.9 |

Number of observations: 180, groups: Subj, 4

Fixed Effects:

| | Estimate | SE | df | t value | Pr(>\|t\|) |
|---|---|---|---|---|---|
| (Intercept) | 195.3 | 21.9 | 3.2 | 8.9 | 0.0024 |
| Cons-Rhotic | 25.7 | 10.7 | 175.0 | 2.4 | 0.0176 |

**Table B5**
TT–TB lag (ms) in Codas.

Random Effects:

| Groups | Name | Variance | S.D. |
|---|---|---|---|
| Subj | (Intercept) | 3166 | 56.3 |
| Residual | | 3201 | 56.6 |

Number of observations: 180, groups: Subj, 4

Fixed Effects:

| | Estimate | SE | df | t value | Pr(>\|t\|) |
|---|---|---|---|---|---|
| (Intercept) | 148.1 | 28.6 | 3.1 | 5.2 | 0.0133 |
| Cons-Rhotic | −70.0 | 8.9 | 175.0 | −7.8 | 4.73e − 13 |

**Table B6**
TB–V lag (ms) in Lateral Codas as a function of Vowel Backness. Vowel quality treatment coded as Back [ʌ-ɑ-oʊ-ʊ-u] = 0; Front [i-ɪ-eɪ-ɛ-æ] = 1.

Random Effects:

| Groups | Name | Variance | S.D. |
|---|---|---|---|
| Subj | (Intercept) | 2360 | 48.6 |
| Residual | | 3457 | 58.8 |

Number of observations: 120, groups: Subj, 4

Fixed Effects:

| | Estimate | SE | df | t value | Pr(>\|t\|) |
|---|---|---|---|---|---|
| (Intercept) | 148.1 | 25.5 | 3.3 | 5.8 | 0.0078 |
| Vfb-Front | 94.4 | 10.7 | 115.0 | 8.8 | 1.66e−14 |

## Appendix C. Summary of statistical modeling: vowel-liquid coarticulatory interaction

Statistics of linear mixed-effects models examining the effects of consonant type and syllable position on lingual dis-

**Table C1**
Coarticulatory Resistance: log lingual displacement of liquids (mm/gridline) as a function of Consonant type (Lat/Rho) and syllable Position (Coda/Ons).

Model: $log(Dist) \sim Con * Pos + (Con|Subj) + (Pos|Subj)$

Random Effects:

| Groups | Name | Variance | S.D. | Corr |
|---|---|---|---|---|
| Subj | (Intercept) | 0.007 | 0.081 | |
| | Con-Rho | 0.052 | 0.228 | −0.61 |
| Subj.1 | (Intercept) | 0.021 | 0.142 | |
| | Pos-Ons | 0.098 | 0.313 | −0.69 |
| Residual | | 0.093 | 0.304 | |

Number of observations: 480, groups: Subj, 4

Fixed Effects:

| | Estimate | SE | df | t-value | Pr(>\|t\|) |
|---|---|---|---|---|---|
| (Intercept) | 0.646 | 0.086 | 2.01 | 7.47 | 0.0172 |
| Con-Rho | −0.407 | 0.121 | 3.35 | −3.37 | 0.0368 |
| Pos-Ons | −0.178 | 0.161 | 3.19 | −1.11 | 0.3452 |
| Con-Rho:Pos-Coda | 0.188 | 0.056 | 467.00 | −3.39 | 0.0008 |

Correlation of Fixed Effects:

| | (Intr) | Con-Rho | Pos-Ons |
|---|---|---|---|
| Con-Rho | −0.343 | | |
| Pos-Ons | −0.606 | 0.040 | |
| Con-Rho:Pos-Ons | 0.161 | −0.230 | −0.172 |

**Table C2**
Coarticulatory Aggression: lingual displacement of vowels (mm/gridline) as a function of Consonant type (Lat/Rho) and syllable Position (Coda/Ons).

Model: $Dist \sim Con * Pos + (Pos|Subj)$

Random Effects:

| Groups | Name | Variance | S.D. | Corr |
|---|---|---|---|---|
| Subj | (Intercept) | 0.035 | 0.187 | |
| | Pos-Ons | 0.048 | 0.218 | −0.95 |
| Residual | | 0.061 | 0.248 | |

Number of observations: 80, groups: Subj, 4

Fixed Effects:

| | Estimate | SE | df | t-value | Pr(>\|t\|) |
|---|---|---|---|---|---|
| (Intercept) | 0.581 | 0.109 | 3.96 | 5.35 | 0.0061 |
| Con-Rho | 0.292 | 0.078 | 70.00 | 3.73 | 0.0004 |
| Pos-Ons | 0.049 | 0.134 | 4.35 | 0.37 | 0.7321 |
| Con-Rho:Pos-Ons | −0.220 | 0.111 | 70.00 | −1.99 | 0.0508 |

Correlation of Fixed Effects:

| | (Intr) | Con-Rho | Pos-Ons |
|---|---|---|---|
| Con-Rho | −0.360 | | |
| Pos-Ons | −0.877 | 0.292 | |
| Con-Rho:Pos-Ons | 0.225 | −0.707 | −0.412 |

placement (Section 3.5) are summarised in Tables C1 and C2. Consonant coding: Lateral = 0, Rhotic = 1. Position coding: Coda = 0, Onset = 1. *p*-values are calculated with the *lmerTest* package (Kuznetsova et al., 2017) using Satterthwaite's method of approximation.

## References


Alwan, A., Narayanan, S., & Haker, K. (1997). Toward articulatory-acoustic models for liquid approximants based on MRI and EPG data. Part II. The rhotics. *The Journal of the Acoustical Society of America, 101*, 1078–1089.

Bates, D., Mächler, M., Bolker, B., & Walker, S. (2015). Fitting linear mixed-effects models using lme4. *Journal of Statistical Software, 667*, 1–48.

Bladon, R. A. W., & Al Bamerni, A. (1976). Coarticulation resistance in English/l/. *Journal of Phonetics, 4*, 137–150.

Bresch, E., Kim, Y.-C., Nayak, K., Byrd, D., & Narayanan, S. (2008). Seeing speech: Capturing vocal tract shaping using real-time magnetic resonance imaging [Exploratory DSP]. *IEEE Signal Processing Magazine, 25*, 123–132.

Bresch, E., Nielsen, J., Nayak, K., & Narayanan, S. (2006). Synchronized and noise-robust audio recordings during realtime magnetic resonance imaging scans. *Journal of the Acoustical Society of America, 120*, 1791–1794.

Browman, C. P., & Goldstein, L. (1988). Some notes on syllable structure in articulatory phonology. *Phonetica, 45*, 140–155.

Browman, C. P., & Goldstein, L. (1995a). Dynamics and articulatory phonology. In T. van Gelder & B. Port (Eds.), *Mind as motion: Explorations in the dynamics of cognition* (pp. 175–193). Cambridge, MA: MIT Press.

Browman, C. P., & Goldstein, L. M. (1986). Towards an articulatory phonology. *Phonology yearbook, 3*, 219–252.

Browman, C. P., & Goldstein, L. M. (1989). Articulatory gestures as phonological units. *Phonology, 6*, 201–251.

Browman, C. P., & Goldstein, L. M. (1992). Articulatory phonology: An overview. *Phonetica, 49*, 155–180.

Browman, C. P., & Goldstein, L. M. (1995b). Gestural syllable position effects in American English. In F. Bell-Berti & L. J. Raphael (Eds.), *Producing speech: Contemporary issues (for Katherine Safford Harris)* (pp. 19–34). New York: AIP Press.

Brunner, J., Geng, C., Sotiropoulou, S., & Gafos, A. (2014). Timing of german onset and word boundary clusters. *Laboratory Phonology, 5*, 403–454.

Brysbaert, M., & Stevens, M. (2018). Power analysis and effect size in mixed effects models: A tutorial. *Journal of Cognition, 1*, 1–20.

Byrd, D. (1996). Influences on articulatory timing in consonant sequences. *Journal of Phonetics, 24*, 209–244.

Byrd, D., Tobin, S., Bresch, E., & Narayanan, S. (2009). Timing effects of syllable structure and stress on nasals: A real-time MRI examination. *Journal of Phonetics, 37*, 97–110.

Chitoran, I., Goldstein, L. M., & Byrd, D. (2002). Gestural overlap and recoverability: Articulatory evidence from Georgian. In C. Gussenhoven & N. Warner (Eds.), *Laboratory phonology 7* (pp. 419–447). Berlin; New York: Mouton de Gruyter.

Delattre, P., & Freeman, D. C. (1968). A dialect study of American r's by x-ray motion picture. *Linguistics, 44*, 29–68.

Espy-Wilson, C. Y., Boyce, S. E., Jackson, M., Narayanan, S., & Alwan, A. (2000). Acoustic modeling of American English /r/. *Journal of the Acoustical Society of America, 108*, 343–356.

Farnetani, E. (1990). Vcv lingual coarticulation and its spatiotemporal domain. In W. Hardcastle & A. Marchal (Eds.), *Speech production and speech modelling* (pp. 93–130). Springer.

Fowler, C. A., & Saltzman, E. (1993). Coordination and coarticulation in speech production. *Language and Speech, 36*, 171–195.

Gick, B. (2003). Articulatory correlates of ambisyllabicity in English glides and liquids. In J. Local, R. Ogden, & R. A. M. Temple (Eds.), *Papers in laboratory phonology VI: Phonetic interpretation* (pp. 222–236). Cambridge; New York: Cambridge University Press.

Gick, B., & Campbell, F. (2003). Intergestural timing in English /r/. In *Proc. 15th Intl. Congress of Phonetic Sciences* (pp. 1911–1914). ICPhS.

Gick, B., Campbell, F., Oh, S., & Tamburri-Watt, L. (2006). Toward universals in the gestural organization of syllables: A cross-linguistic study of liquids. *Journal of Phonetics, 34*, 49–72.

Gick, B., Iskarous, K., Whalen, D. H., & Goldstein, L. M. (2003). Constraints on variations in the production of English /r/. In *6th international seminar on speech production* (pp. 73–78). Sydney: ISSP.

Giegerich, H. J. (1992). *English phonology: An introduction*. Cambridge Univ Press.

Giles, S. B., & Moll, K. L. (1975). Cinefluorographic study of selected allophones of English/l/. *Phonetica, 31*, 206–227.

Green, P., & MacLeod, C. J. (2016). SIMR: An R package for power analysis of generalized linear mixed models by simulation. *Methods in Ecology and Evolution, 7*, 493–498.

Hagiwara, R. (1994). Three types of American/r/. In *UCLA working papers in phonetics* (pp. 55–62).

Hammond, M. (1999). *The phonology of English: A prosodic optimality-theoretic approach*. Oxford; New York: Oxford Univ. Press.

Hardcastle, W. J., & Barry, W. (1989). Articulatory and perceptual factors in/l/ vocalisations in english. *Journal of the International Phonetic Association, 15*, 3–17.

Kenyon, J. S., & Knott, T. A. (1953). *A pronouncing dictionary of American English*. Mass: Merriam Springfield.

Kirby, J., & Sonderegger, M. (2018). Mixed-effects design analysis for experimental phonetics. *Journal of Phonetics, 70*, 70–85.

Krakow, R. A. (1999). Physiological organization of syllables: A review. *Journal of Phonetics, 27*, 23–54.

Kuznetsova, A., Brockhoff, P. B., & Christensen, R. H. B. (2017). lmerTest package: Tests in linear mixed effects models. *Journal of Statistical Software, 82*, 1–26.

Labov, W., Ash, S., & Boberg, C. (2005). *The atlas of North American English: Phonetics, phonology and sound change*. Walter de Gruyter.

Lee-Kim, S.-I., Davidson, L., & Hwang, S. (2013). Morphological effects on the darkness of English intervocalic /l/. *Laboratory Phonology, 4*, 475–511.

Leidner, D. R. (1976). The articulation of American English /l/: A study of gestural synergy and antagonism. *Journal of Phonetics, 4*, 327–335.

Lin, S., Davies, B., Turpin, M., Ross, A., & Demuth, K. (2014). The articulation of kaytetye coronals. In *Proc. 14th conf. on laboratory phonology.* National Institute for Japanese Linguistics Tokyo: NINJAL.

Lindau, M. (1985). The story of /r/. In V. Fromkin (Ed.), *Phonetic linguistics: Essays in honor of Peter Ladefoged* (pp. 157–168). Orlando: Academic Press.

Lingala, S. G., Zhu, Y., Kim, Y.-C., Toutios, A., Narayanan, S., & Nayak, K. S. (2017). A fast and flexible MRI system for the study of dynamic vocal tract shaping. *Magnetic Resonance in Medicine, 77*, 112–125.

Marin, S. (2013). The temporal organization of complex onsets and codas in Romanian: A gestural approach. *Journal of Phonetics, 41*, 211–227.

Marin, S., & Pouplier, M. (2010). Temporal organization of complex onsets and codas in american english: Testing the predictions of a gestural coupling model. *Motor Control, 14*, 380–407.

Nam, H., Goldstein, L., Browman, C., Rubin, P., Proctor, M., & Saltzman, E. (2006). Tada (task dynamics application) manual..

Nam, H., Goldstein, L., Saltzman, E., & Byrd, D. (2004). Tada: An enhanced, portable task dynamics model in matlab. *Journal of the Acoustical Society of America, 115, 2430*. URL:http://adsabs.harvard.edu/abs/2001ASAJ.115.2430N.

Mielke, J., Baker, A., & Archangeli, D. (2016). Individual-level contact limits phonological complexity: Evidence from bunched and retroflex /r/. *Language, 92*, 101–140.

Nam, H., Goldstein, L. M., & Saltzman, E. L. (2009). Self-organization of syllable structure: A coupled oscillator model. In I. Chitoran, C. Coupé, E. Marisco, & F. Pellegrino (Eds.), *Approaches to phonological complexity* (pp. 299–328). Berlin: Mouton.

Narayanan, S., Nayak, K., Lee, S., Sethy, A., & Byrd, D. (2004). An approach to real-time magnetic resonance imaging for speech production. *Journal of the Acoustical Society of America, 115*, 1771–1776.

Narayanan, S., Toutios, A., Ramanarayanan, V., Lammert, A., Kim, J., Lee, S., et al. (2014). Real-time magnetic resonance imaging and electromagnetic articulography database for speech production research (TC). *Journal of the Acoustical Society of America, 136*, 1307–1311.

Narayanan, S. S., Alwan, A. A., & Haker, K. (1997). Toward articulatory-acoustic models for liquid approximants based on MRI and EPG data. Part I. The laterals. *The Journal of the Acoustical Society of America, 101*, 1064–1077.

Pastätter, M., & Pouplier, M. (2017). Articulatory mechanisms underlying onset-vowel organization. *Journal of Phonetics, 65*, 1–14.

Pouplier, M. (2012). The gestural approach to syllable structure: Universal, language- and cluster-specific aspects. In S. Fuchs, M. Weirich, D. Pape, & P. Perrier (Eds.), *Speech planning and dynamics* (pp. 63–96). Peter Lang Verlag Frankfurt am Main.

Proctor, M. (2011). Towards a gestural characterization of liquids: Evidence from Spanish and Russian. *Laboratory Phonology, 2*, 451–485.

Proctor, M., Lo, C., & Narayanan, S. (2015). Articulation of English vowels in running speech: A real-time MRI study. In *Proc. Int'l congress on phonetic sciences*. . Glasgow.

Proctor, M., & Walker, R. (2012). Articulatory bases of English liquids. In S. Parker (Ed.), The Sonority Controversy (pp. 285–312). Berlin: De Gruyter volume 18 of Studies in Generative Grammar..

Proctor, M. I., Bone, D., & Narayanan, S. S. (2010). Rapid semi-automatic segmentation of real-time Magnetic Resonance Images for parametric vocal tract analysis. In *Proc. Int'l conf. on speech communication and technology* (pp. 1576–1579). Makuhari, Japan.

Proctor, M. I., Katsamanis, N., Goldstein, L., Hagedorn, C., Lammert, A., & Narayanan, S. (2011). Direct estimation of articulatory dynamics from real-time Magnetic Resonance Image sequences. In *Proc. Int'l conf. on speech communication and technology* (pp. 281–284). Florence, Italy.

R Core Team (2018). R: A Language and Environment for Statistical Computing. R Foundation for Statistical Computing Vienna, Austria. URL:https://www.R-project.org/..

Recasens, D. (1984). V-to-C coarticulation in catalan VCV sequences: An articulatory and acoustical study. *Journal of Phonetics, 12*, 61–73.

Recasens, D., & Espinosa, A. (2009). An articulatory investigation of lingual coarticulatory resistance and aggressiveness for consonants and vowels in Catalan. *Journal of the Acoustical Society of America, 125*, 2288–2298.

Recasens, D., Pallarès, M. D., & Fontdevila, J. (1997). A model of lingual coarticulation based on articulatory constraints. *Journal of the Acoustical Society of America, 102*, 544–561.

Recasens, D., & Rodríguez, C. (2016). A study on coarticulatory resistance and aggressiveness for front lingual consonants and vowels using ultrasound. *Journal of Phonetics, 59*, 58–75.

Recasens, D., & Rodríguez, C. (2017). Lingual articulation and coarticulation for catalan consonants and vowels: An ultrasound study. *Phonetica, 74*, 125–156.

Saltzman, E. L., & Munhall, K. G. (1989). A dynamical approach to gestural patterning in speech production. *Ecological Psychology, 1*, 333–382.

Saltzman, E. L., Rubin, P. E., Goldstein, L., & Browman, C. P. (1987). Task-dynamic modeling of interarticulator coordination. *Journal of the Acoustical Society of America, 82*, S15.

Scobbie, J. M., & Pouplier, M. (2010). The role of syllable structure in external sandhi: An EPG study of vocalisation and retraction in word-final English /l/. *Journal of Phonetics, 38*, 240–259.

Sproat, R., & Fujimura, O. (1993). Allophonic variation in English/l/ and its implications for phonetic implementation. *Journal of Phonetics, 21*, 291–311.

Tilsen, S. (2016). Selection and coordination: The articulatory basis for the emergence of phonological structure. *Journal of Phonetics, 55*, 53–77.

Uldall, E. T. (1958). American 'molar' r and 'flapped' r. *Revista do Laboratorio de Fone'tica Experimental (Coimbra), 4*, 103–106.

Walker, R., & Proctor, M. (2013). Articulatory overlap in English syllables with postvocalic /ɹ/. *Proceedings of Meetings on Acoustics, 19* 060259.

Walker, R., & Proctor, M. (2019). The organisation and structure of rhotics in American English rhymes. *Phonology, 36*(3), 457–495.

Wells, J. (2008). *Longman pronunciation dictionary*. Pearson Education India.

Wells, J. C. (1982). Accents of English. In *Vol 1: An introduction volume 1*. Cambridge: Cambridge Univ. Press.

Westfall, J., Kenny, D. A., & Judd, C. M. (2014). Statistical power and optimal design in experiments in which samples of participants respond to samples of stimuli. *Journal of Experimental Psychology: General, 143*, 2020–2045.

Ying, J., Carignan, C., Shaw, J.A., Proctor, M., Derrick, D., & Best, C.T. (2017). Temporal Dynamics of Lateral Channel Formation in/l/: 3D EMA Data from Australian English. (pp. 2978–2982)..

Zawadzki, P. A., & Kuehn, D. P. (1980). A cinereadiographic study of static and dynamic aspects of American English /r/. *Phonetica, 37*, 253–266.

Zhou, X., Espy-Wilson, C. Y., Boyce, S., Tiede, M., Holland, C., & Choe, A. (2008). A magnetic resonance imaging-based articulatory and acoustic study of 'retroflex' and 'bunched' American English/r/. *Journal of the Acoustical Society of America, 123*, 4466–4481.

Zhu, Y., Kim, Y.-C., Proctor, M. I., Narayanan, S., & Nayak, K. S. (2013). Dynamic 3D visualization of vocal tract shaping during speech. *IEEE Transactions on Medical Imaging, 32*, 838–848.